The Pennsylvania State University

The Graduate School

CHARACTERIZATION OF TUMOR GROWTH, IMMUNE AND METASTATIC OUTCOMES IN THE 4T1.2-HER2 MAMMARY TUMOR MODEL

A Thesis in

Integrative and Biomedical Physiology

by

Abirami Ravichandran

Submitted in Partial Fulfillment
of the Requirements
for the Degree of

Master of Science

August 2021

The thesis of Abirami Ravichandran was reviewed and approved by the following:

Connie J. Rogers

Associate Professor of Nutritional Sciences and Physiology

Thesis Advisor

Margherita T. Cantorna

Distinguished Professor of Molecular Immunology and Nutrition

Robert F. Paulson

Professor of Veterinary and Biomedical Sciences

Donna H. Korzick

Professor of Physiology and Kinesiology

Chair, Integrative and Biomedical Physiology

ABSTRACT

In 2020, breast cancer surpassed lung cancer to become the most prevalent type of cancer worldwide. Breast cancer is the leading cause of cancer-related mortality in women. The main contributing factor for death in breast cancer is metastatic disease. Mouse models are an excellent tool for mechanistic studies pertaining to breast cancer. 4T1.2 mouse mammary tumor model with triple-negative phenotype and clinically relevant metastatic properties has been used in many preclinical breast cancer studies. However, 4T1.2 has no known tumor antigens and is poorly immunogenic, limiting the use of this model in immunological studies.

To overcome this drawback, in the 4T1.2-HER2 tumor cell, the parental 4T1.2 tumor cell has been modified to stably express the surrogate antigen, HER2. HER2 is used as the tumor antigen in this breast cancer model. When implanted *in vivo* in BALB/c mice, tumor growth of the 4T1.2-HER2 tumor was significantly different from the parental tumor model. It exhibited a short period of initial tumor growth followed by spontaneous tumor regression, which was dependent on the adaptive immune response. Following the regression phase, in the third phase, a subset of mice demonstrated tumor outgrowth, whereas others rejected the tumor. Experiments were undertaken in our laboratory to characterize the immune responses in the early phases of tumor growth and regression. In the early phases, tumor growth was associated with a decrease in T cells and an increase in myeloid-derived suppressor cells (MDSCs), whereas tumor regression was associated with an increase in T cells and a decrease in MDSCs in the spleen and tumor. Moreover, HER2-specific IFNγ secretion from splenic and tumor-infiltrating immune cells was evident during the tumor regression period.

The goal of the present study was to characterize the tumor growth, immune responses, and metastatic outcomes in the 4T1.2-HER2 mammary tumor model during the late stages of tumor growth. In the 4T1.2-HER2 tumor model, considerable heterogeneity was observed in the tumor volume of mice during the third phase of tumor growth. Since the mice had varying tumor volumes in the third phase of tumor growth, for aim 1, we wanted to determine if tumor volume was associated with immune cell populations in the spleen and tumor. In the spleen, the percentage of dendritic cells and Tregs were negatively associated, and the percentage of MDSCs and monocytic MDSCs were positively associated with tumor volume. In the tumors, the percentage of CD4, NK cells, Tregs, and central memory T cells were negatively associated with tumor volumes, whereas MDSCs, effector memory cells, and memory precursor effector cells were positively associated with tumor volume.

Subsequently, we wanted to examine if the tumor volume was associated with antigen-specific immune responses against HER2 in the spleen and tumor. Stimulation of immune cells from spleen and tumor using H-2K^{d}-restricted HER2 peptide induced IFNγ secretion from the tumor-infiltrating lymphocytes (TILs) but not from the splenocytes. Further, IFNγ secretion from the TILs was significant only in smaller-sized tumors.

For aim 3, we wanted to determine if tumor volume was associated with lung metastatic burden. Using the gene expression of gp70, we observed that all the mice had lung metastasis. However, no significant difference was seen in the lung metastatic burden between the mice with larger tumor volumes and smaller tumor volumes.

From this study, we observed associations between the immune cell populations in the spleen and tumor and the tumor volume. Further, we could also observe a significant HER2-specific immune response in smaller tumors. In conclusion, with the introduction of the surrogate tumor antigen, HER2, in the 4T1.2 tumor cells, *in vivo* immunogenicity is increased, and HER2-specific immune responses are induced in the tumor. These immune features are highly preferred in a tumor model for immunological studies. This model would be an ideal experimental system for exploring questions related to the effect of interventions on antigen-specific immune responses against tumors in a preclinical setting.

TABLE OF CONTENTS

LIST OF FIGURES

LIST OF TABLES

LIST OF ABBREVIATIONS

Ab	Antibody
ADCC	Antibody-dependent cell-mediated cytotoxicity
APC	Antigen-presenting cell
BCR	B cell receptor
BSA	Bovine serum albumin
CD	Cluster of differentiation
cDNA	complementary Deoxyribonucleic acid
CER	Continuous energy restriction
CM	Complete Medium
CTL	Cytotoxic T lymphocytes
DC	Dendritic cell
DCIS	Ductal carcinoma in situ
DMEM	Dulbecco's Modified Eagle Medium
DNA	Deoxyribonucleic acid
DPEC	Double-positive effector cells
EEC	Early effector cells
ELISA	Enzyme-linked immunosorbent assay
ER	Estrogen receptor
FDA	Food and Drug Administration
gMDSC	Granulocytic myeloid-derived suppressor cell
h	hour/hours
HA	Hemagglutinin
HER2	Human Epidermal growth factor Receptor 2
IER	Intermittent energy restriction
IF	Intermittent fasting
IFNγ	Interferon-γ
Ig	Immunoglobulin
IGF	Insulin-like growth factor
IL	Interleukin
iNOS	Inducible nitric oxide synthase
LCIS	Lobular carcinoma in situ
MDSC	Myeloid-derived suppressor cell
MHC	Major histocompatibility complex
mMDSC	monocytic myeloid-derived suppressor cell
MPEC	Memory precursor effector cells
mRNA	Messenger Ribonucleic acid
NK	Natural killer cell
NO	Nitric oxide
PBS	Phosphate-buffered saline
PCR	Polymerase Chain Reaction
pCR	Pathological complete response
PD-1	Programmed cell death protein-1
pDC	plasmacytoid dendritic cells
PD-L1	Programmed death-ligand 1
PR	Progesterone receptor

RNA	Ribonucleic acid
ROS	Reactive oxygen species
RPMI	Roswell Park Memorial Institute
SD	Standard deviation
SEM	Standard error of mean
SERM	Selective estrogen receptor modulator
SHBG	Sex hormone-binding globulin
SLEC	Short-lived effector cells
TCM	Central memory T cells
TCR	T cell receptor
TDLU	Terminal ductal lobular unit
TEM	Effector memory cells
TH	T helper cells
TIL	Tumor-infiltrating lymphocytes
TME	Tumor microenvironment
TNBC	Triple-negative breast cancer
Treg	Regulatory T cell
WHO	World Health Organization

ACKNOWLEDGEMENTS

First and foremost, I would like to express my sincerest gratitude to my advisor, Dr. Connie Rogers for her guidance and mentorship. Her insights, support, and encouragement have greatly helped my personal and professional development.

I would like to thank my committee members, Dr. Cantorna and Dr. Paulson for taking their time amidst their busy schedules to help with my thesis and for giving invaluable advice and feedback.

I am grateful to my lab mates at Rogers Lab, Yitong (Sherry) Xu, Ester Oh, Janhavi Damani, Abriana Cain, and Emily bean for their help and encouragement. They make my graduate experience enjoyable. I would like to thank Sherry particularly for teaching me the experimental techniques.

I would like to thank my family for being my pillars of strength and supporting me in all my endeavors. My parents, Geetha and Ravichandran, my brother, Arun, my sister-in-law, Vidhya, my husband, Raghav, and my parents-in-law, Usha and Ramesh, have always provided unconditional love and support, and I feel blessed to have such a family. Special thanks to my husband for making State College his home and taking every effort to support my career. I would also like to thank all my friends here at Penn State for their support and company.

CHAPTER 1: LITERATURE REVIEW

1.1. INTRODUCTION

Malignant neoplasm, commonly referred to as cancer, is a disease characterized by uncontrolled proliferation of cells with tissue invasion (1). Globally, cancer is the second leading cause of death worldwide after ischemic heart disease, with one in every six persons dying due to cancer (2). Cancer is expected to surpass ischemic heart disease as the leading cause of death by 2060 (3). Cancer not only impacts the survival of the affected individual but also dramatically reduces the quality of life. As a direct result of the disease and from the side effects due to various treatments, patients suffer physiologically as well as psychologically (4). Further, the medical expenses that arise due to cancer treatment and rehabilitation impact the affected individual as well as the family financially. Worldwide, the expenses incurred due to cancer are said to be in billions of dollars per year (5). Cancer is a major public health problem affecting millions of people's lives and livelihoods every year, and new strategies need to be developed to prevent and treat malignancies and their recurrences.

1.2. BREAST CANCER

1.2.1. Epidemiological data

Breast cancer is the most common cancer type in the United States (6). With over 276,000 estimated new cases, breast cancer accounted for 15.3% of overall cancer incidence in the United States in 2020 (6). Estimates by WHO from 2020

indicate that breast cancer surpassed lung cancer to become the most commonly diagnosed cancer worldwide with 2.25 million cases which constitute nearly 11.7% of the overall cancer incidence (7). Breast cancer is the leading cause of cancer-related death in women worldwide and the second leading cause of cancer-related deaths in the United States with 684,996 and 42,170 estimated deaths worldwide and in the United States, respectively (6, 7). The numbers are high despite the widespread awareness about breast cancer screening and advances in cancer diagnostic technologies and therapy. The survival rates have increased marginally over the last three decades, with a current 5-year overall survival rate of 90% due to screening, early detection, and therapeutic advances. However, the outcomes are still poor for metastatic and recurrent breast cancer cases. The treatment for such cases is associated with many side effects, and treatment resistance is observed in many patients (6). There is a need to increase our understanding of the mechanisms underlying risk factors, preventive and therapeutic strategies to manage metastatic disease.

1.2.2. Anatomy and histology of the mammary gland

Breast tissue is composed of a mass of glandular tissue, also known as corpus mammae, supported by connective tissue and covered by a thick layer of mammary adipose tissue (8, 9). The glandular tissue is made up of lactiferous ducts and terminal ductal lobar units (TDLU). The major duct systems radiate from the nipple. They ramify to form the lobes and lobules, about 15-20 and 20-40 of them respectively, in each breast. The ducts end in terminal ductal lobar units (TDLU), which are the functional units of the breast and the sites of milk production in lactating women (10, 11). The majority of breast lesions arise from TDLU (12). The ducts and TDLU are made up of

luminal epithelial cells, which are cuboidal to columnar in shape. The expression of hormonal receptors (estrogen and progesterone receptors) is usually found on the ductal system and TDLU but not on proliferating luminal epithelial cells. The TDLU are surrounded by myoepithelial cells, which contain smooth muscle cell properties and help in milk ejection (10). In addition to the two types of epithelial cells - luminal and myoepithelial, epithelial progenitor cells may be present. These progenitors are known as basal cells and can give rise to luminal and myoepithelial cells (13). The stroma of the breast is composed of fibrous and adipose tissue. The breast, as a tissue, undergoes continuous changes in response to menarche, pregnancy, lactation, and menopause (8, 10).

1.2.3. Classification of breast cancer

Breast cancers exhibit diversity in terms of their morphologies and molecular properties. A number of subtypes have been characterized with varied clinical presentation, different disease progression patterns, and diverse responses to therapy and prognostic outcomes (14). Breast cancer has been classified into subtypes based on histopathological characteristics and immunohistochemical or molecular characteristics (15).

Adenocarcinoma is the most common histological presentation of breast cancer (95%). WHO recognizes nearly 21 types of breast cancer based on histological patterns (14, 15). The origin of breast cancer is usually from the TDLU, and it can originate from either of the epithelial cell types. Broadly, breast cancer can be classified into ductal or lobular carcinoma. Both ductal and locular carcinoma could be confined in the epithelial layer (*in situ*) as ductal carcinoma *in situ* (DCIS) and lobular carcinoma *in situ* (LCIS) or spread invasively as invasive ductal carcinoma and

invasive lobular carcinoma (14). Invasive ductal carcinoma and invasive lobular carcinoma represent nearly 80% and 10%, respectively, of all invasive breast cancers (16). Invasive carcinomata of both types are further divided into many subtypes. Of the histological subtypes, an invasive ductal carcinoma subtype called invasive ductal carcinoma no specific type (NST) is the most common type of all breast cancers, and it constitutes nearly 40-75% of all invasive breast cancers (14). The histological classification of breast cancer is routinely used in clinical settings and is helpful to predict the behavior and prognosis of tumors.

Breast cancers can be assessed for the expression of molecules such as estrogen receptor (ER), progesterone receptor (PR), human epidermal growth factor receptor 2 (HER2), also known as c-ErbB-2, cytokeratin, and proliferation marker, Ki-67 (14-16). Using the molecular expression profile, breast cancers can be classified into molecular subtypes as luminal A, luminal B, HER2-enriched, and basal-like breast cancers. Luminal A is ER/PR positive and HER2 low expressing subtype. It is the most common molecular subtype of breast cancer with an incidence of 28%-31%, and it has a good prognosis (14, 15). Luminal B subtype is ER/PR positive and HER2 positive. This subtype is found in 20% of breast cancer (16). It is of a higher grade than Luminal A (Ki-67 level is 14% or more), and its prognosis is poorer than Luminal A (14). HER2 overexpression subtype is ER/PR negative and HER2 strong positive. This accounts for 17% of all breast cancers. Ki-67 expression is high, and this subtype has a poor prognosis. However, this subtype is responsive to HER2 receptor-based treatments such as trastuzumab (Herceptin) (14, 16). Basal-like breast cancers are ER/PR negative and HER2 negative. Due to the absence of ER, PR, and HER2, they are also called triple-negative breast cancer (TNBC). The incidence of TNBC is about 15% of all breast cancers. They have a high expression of Ki-67 and have high proliferation

rates with poor outcomes (14-16). Molecular classification of breast cancer is particularly helpful for designing therapeutic strategies (14).

1.2.4. Staging of breast cancer

Stage of breast cancer defines how advanced a patient's cancer is in terms of primary tumor sizes (T), lymph node involvement (N), and metastasis (M). This staging is also called the TNM system of staging. The scores are given for the clinical features of a patient's cancer with the following ranges: T stage (T0-T4), N stage (N0-N3), and M stage (M0-M1). These scores are combined to give an overall score for the patient's cancer stage (stage 0-IV). For each scoring range, a higher score implies a more severe or advanced pathology (1, 17). TNM staging is an excellent prognostic tool, and it is very helpful for designing treatment strategies for a patient. Based on TNM staging, the 5-year relative survival rate is 98.9% for localized breast cancer (Stage I) and 28.1% for metastatic breast cancer (Stage IV) (1, 6).

1.2.5. Etiology and risk factors

Breast cancer is considered to be a disease of multifactorial etiology. Studies have identified many risk factors which influence breast cancer, including sex, ageing, genes and family history, age at menarche and menopause, history of breast disease, breast density, exogenous hormones, female reproductive factors, obesity, and lifestyle factors such as diet, alcohol, physical inactivity (18, 19). These factors could be classified as modifiable and non-modifiable factors.

1.2.5.1. Non-modifiable risk factors

Age, sex, race, genetic factors, age at menopause and menarche, and pre-existing breast conditions are some of the known non-modifiable risk factors. Breast

cancer is 100 times more common in females than in males, and therefore, female sex is an important risk factor for breast cancer (19). Cancer is an age-associated disease. Ageing increases the risk of breast cancer as well, but certain hormonal factors make the age-associated incidence pattern to be unique for breast cancer. The incidence of breast cancer increases after the age of 20 years because of the exposure of breast tissues to ovarian hormones. Compared to other epithelial cancers whose incidence starts increasing at a later age, usually 40, the age of incidence for breast cancer is sooner (19, 20). The incidence of breast cancer continues to rise rapidly till the age of 35-40 years. After 40 years, the incidence by age differs between various countries. In countries such as the United States, Denmark, and Iceland, the incidence increases until the age of 70. In contrast, in countries like Japan, Columbia, and Thailand, the incidence stops increasing or declines after the age of 45 (19, 21, 22). In the countries with increasing incidence after 40 years, an associated increase in average body weight is also observed. It is hypothesized that increased average body weight with greater adipose could cause increased estrogen secretion, which in turn causes an increased incidence of breast cancer. Further, menopause also occurs later in women in countries like the United States, and that could also be related to the increased incidence (19). Incidence of breast cancer before the age of 40 is associated with a higher grade of cancer, later stage at diagnosis, and poor survival outcomes compared to the incidence in older women. Triple-negative phenotype is common among younger women than older women (23).

Family history is a well-established risk factor for breast cancer. Women with a first-degree relative diagnosed with breast cancer have a two-fold higher risk. Certain genetic mutations have been associated with an increased risk of breast cancer. Mutations associated with tumor suppressor BRCA genes, BRCA1 and BRCA2, are

the most common among them, and females who possess BRCA gene mutation have anywhere between 40%-70% chance of developing breast cancer (18-20, 24). Genetic polymorphism of genes involved in estrogen synthesis or estrogen metabolism, which may make the subject more susceptible to the effects of substances such as estrogen, alcohol is associated with increased breast cancer risk (18, 19, 25).

Women with a history of breast diseases such as atypical epithelial hyperplasia have a higher risk of breast cancer (19, 20). Breast or mammographic density refers to non-radiolucent portions of a mammograph that correspond to the glandular and fibrous tissues in the breast. Women with greater breast density have a four-fold risk of breast cancer (18, 19).

Early menarche and delayed menopause increase the risk of breast cancer. Younger age at menopause by natural as well as surgical causes reduces the risk of breast cancer (18, 19, 26). Early menarche or late menopause can considerably increase the duration of exposure to estrogen, which increases breast cancer risk (19, 26).

1.2.5.2. Modifiable risk factors

Modifiable risk factors include lifestyle factors such as diet, alcohol, physical inactivity, obesity, certain modifiable reproductive factors, and use of exogenous hormones (18, 27). Nulliparity increases the risk of breast cancer. Each childbirth reduces breast cancer risk by 3% for premenopausal breast cancer and 12% for postmenopausal breast cancer (26). However, first pregnancy at an older age (>35 years) is associated with increased breast cancer risk compared to nulliparous women (21). Breastfeeding is associated with protective effects in breast cancer, particularly the premenopausal type. Longer duration of breastfeeding results in delayed ovulation

and altered hormonal levels with increased prolactin and decreased estrogen, which could exert protective effects (18, 19, 26, 28). Exposure to exogenous estrogen through the use of hormonal therapy containing estrogen or estrogen and progesterone during the menopausal or postmenopausal period could increase the risk of breast cancer (19, 20, 24). Alcohol intake is associated with an increased risk of breast cancer (18, 19). Diet containing soy or carotenoids is associated with decreased breast cancer risk (19, 29).

The association between obesity and breast cancer varies by menopausal status and life stages. Obesity increases the risk of postmenopausal breast cancer, particularly hormonal positive subtypes, while the evidence is on the contrary for premenopausal ER-positive subtype (30). Abdominal obesity, also known as central obesity, increases the risk of triple-negative breast cancer in younger women (30). Obesity causes an increase in estrogen production by increasing aromatase expression, thereby increasing the risk of ER+ breast cancer. Obesity is associated with features such as hyperinsulinemia, insulin resistance, increased IGF-1 levels, elevated inflammatory markers such as C-reactive protein, IL-1, IL-6, TNF-α, altered microbiome, which increase breast cancer risk (30, 31).

Preventive efforts taken against obesity via dietary and physical activity-based interventions could protect against breast cancer risk and improve survival. The beneficial effects of these interventions in breast cancer could be dependent as well as independent of the weight loss caused in subjects. Women's Health Initiative Observational Study found that weight loss (>5% body weight) alone was beneficial in reducing obesity-related breast cancer risk (32). Nurses' Health Study found that >5 kg weight loss after the age of 18 is associated with decreased risk of breast cancer

(33). Data from studies linking bariatric surgery and breast cancer also support the findings from weight loss studies (34).

Physical activity is associated with reduced risk, increased survival rate, and reduced recurrence in breast cancer (35, 36). From a meta-analysis of 31 prospective studies, it was found that physical activity was inversely associated with breast cancer risk, particularly in premenopausal women for estrogen and progesterone receptor-negative breast cancer. Further, a dose-response analysis suggested a reduction in risk of breast cancer by 2% for every 25 metabolic equivalent (MET)-h/week increment in non-occupational physical activity (roughly equivalent to 10 h/week of light household activity) (37). Physical activity may act through mechanisms involving regulation of adiposity, sex hormones including estrogen and androgen, insulin resistance, insulin levels and IGF-1, adipokines, inflammatory markers, immune responses, and prevention of carcinogenesis and angiogenesis (38, 39). A 6-month randomized controlled trial of aerobic exercise on breast cancer survivors showed a reduction in insulin and IGF-1 (40). In a study with postmenopausal breast cancer patients, physical activity increased T cell and NK cell function (41). Many preclinical studies have studied the effects of physical activity on breast cancer using mouse models on treadmills, running wheels, or swimming. The majority of the studies observed beneficial effects of physical activity on breast cancer outcomes, including reduced tumor incidence, tumor growth, metastasis, and improved survival. Studies have also reported changes in the immune responses as a result of PA, but the mechanisms of how physical activity modulates immune response are still being explored (42, 43).

Another potential strategy for reducing breast cancer risk is dietary energy restriction. In many animal studies, calorie restriction has been suggested to reduce breast cancer incidence, metastasis and prolong survival (42, 44). Mechanisms through which energy restriction could potentially exert its beneficial effects systemically include favorable alterations in insulin, IGF-1, leptin, sex hormone-binding globulin (SHBG), estradiol, testosterone, reactive oxygen species (ROS), and increasing adiponectin and IL-6 (45). Besides these mechanisms, energy restriction could also increase autophagy and induce favorable changes in immune responses in the context of cancer, thereby exerting a better prognosis (42). In the 4T1.2 mouse model of breast cancer, calorie restriction has been effective in reducing metastasis and immunosuppression in the tumor microenvironment (TME) (43). Energy restriction could be attained via a continuous energy restriction (CER), intermittent energy restriction (IER), or intermittent fasting (IF). Mechanisms through which each of these energy restriction patterns act may differ from each other. Though IER has been shown to be better than CER in one spontaneous model of breast cancer (44), additional studies are necessary to determine the consistency of these findings. Human breast cancer studies with ER had been undertaken concurrently with weight loss studies, thereby complicating the study of ER effects alone in breast cancer (42, 44, 45). Additional clinical studies are needed to understand the association of energy restriction with breast cancer and the mechanisms involved.

1.2.6. Therapeutic strategies

Treatment options for breast cancer include surgery, radiotherapy, chemotherapy, endocrine therapy, and immunotherapy (1, 46). Surgical procedures involve either breast-conserving surgery or mastectomy. Surgery is sometimes

performed along with the removal of lymph nodes when indicated. For chemotherapy in breast cancer, drugs such as anthracyclines and taxanes are used (46, 47). Radiotherapy can be delivered to a portion of the breast, to the entire breast, or to the chest wall based on the extent of tumor involvement. Endocrine therapy is used in ER-positive breast cancers and the drugs used include selective estrogen receptor modulators (SERMs), aromatase inhibitors, and gonadotropin-releasing hormone agonists (46, 47). Immunotherapy is emerging as a promising treatment option. A wide range of immunotherapeutic strategies is being tested in breast cancer, including blockade of immune checkpoints, antitumor vaccines, regulatory T cell blockade, adoptive T cell transfer therapy, and adoptive immunotherapy with monoclonal antibodies (48). Of these, monoclonal antibody therapy using trastuzumab (commercial name: Herceptin) was approved by FDA in 1998 (49). Trastuzumab is a monoclonal antibody against HER2 and is used clinically as a targeted therapy to treat HER2-positive breast cancer. Studies have shown that trastuzumab causes downregulation of HER2-dependent pathways as well as stimulates antibody-dependent cytotoxic killing of cancer cells (50, 51). In 2019, FDA approved the use of the first immune checkpoint inhibitor for breast cancer, an anti-PD-L1 antibody, atezolizumab (commercial name: Tecentriq), in combination with chemotherapy for the treatment of triple-negative, metastatic breast cancers with positive PD-L1 protein expression (49). PD-1 is a checkpoint protein expressed on the surface of T cells. PD-L1 is the ligand for PD-1, which is expressed in normal cells but overexpressed in some cancers. PD-L1 binds to PD-1 in effector T cells which causes apoptosis in the latter. PD-L1 antibodies block this interaction and enhance T cell responses (52). Despite the promising immunotherapy and chemotherapy combination strategy, this regimen has modest response rates and serious side effects have caused

discontinuation of this therapy in some patients (49). Further studies are needed to employ more immunotherapeutic regimens in routine clinical practice.

Treatment strategy in breast cancer mainly depends on factors such as the cancer type, TNM stage of cancer, the presence of ER, PR, or HER2 receptors, patient's age, menopausal status, and risk vs. benefit of treatment (1, 46). With regards to stage 0 cancers (*in situ* cancers), for LCIS, no treatment but enhanced surveillance is indicated, and for DCIS, breast-conserving surgery and post-surgery radiotherapy are indicated. For early invasive breast cancers (stage I and II), either breast-conserving surgery with radiotherapy or mastectomy is the standard treatment protocol. Systemic adjuvant therapies, including chemotherapy or endocrine therapy for ER positive cancers or anti-HER2 monoclonal antibody therapy (Herceptin/Trastuzumab) for HER2 positive cancers, are also recommended. For locally advanced cancers (stage III), induction chemotherapy to reduce the size of tumors followed by surgery with axillary lymph node dissection (if necessary) along with radiation therapy and adjuvant therapy are indicated. For stage IV or metastatic breast cancer, treatment depends on the patient's goals with the aims of prolonging life and palliative care. The primary tumor is treated by surgery, radiotherapy, or both, along with chemotherapy, hormonal therapy, or targeted therapy based on the cancer type. For palliative therapy, drugs such as bisphosphonates are used to reduce bony complications (1, 46, 47).

1.3. IMMUNE SYSTEM

The immune system is a coordinated group of cells, tissues, and organs that make up the host's defense organization. The immune system protects against a

variety of harmful agents such as pathogens, toxins, or transformed cells by mounting appropriate immune responses. With the exception of certain tissue-resident macrophages, immune cells are derived mainly from the hematopoietic stem cells in the bone marrow (52). The immune system can be classified into two main arms of defense – innate and adaptive immunity (52, 53).

1.3.1. Innate immunity

Innate immunity is the first line of defense against invading pathogens and tumor cells (53, 54). Innate immunity is present at birth because innate immune responses are germline-encoded (55). Innate immune responses can be activated rapidly. The innate immune system includes anatomic barriers such as skin and mucous membranes and physiological parameters such as temperature, pH, and oxygen levels which provide primary protection. Innate immunity also includes complex yet non-specific defense mechanisms such as enzymes, antimicrobial peptides, cytokines, inflammatory mediators, and complement system. These components can prevent the entry of pathogens, eliminate pathogens, or stimulate an inflammatory response (53, 55). Cellular components of the innate immune system include neutrophils, eosinophils, basophils, mast cells, myeloid-derived suppressor cells (MDSCs) and macrophages (and their earlier form, monocytes) from the myeloid lineage, natural killer (NK) cells from the lymphoid lineage and dendritic cells (DCs) which are predominantly from the myeloid lineage but some DCs arise from lymphoid precursors as well (52, 53, 55, 56). Neutrophils, basophils, and eosinophils are also called granulocytes as they contain cytoplasmic granules containing enzymes or microbicidal substances (52). Eosinophils, basophils, and mast cells defend against parasitic infections and mediate allergic responses (53, 55). Neutrophils,

macrophages, and dendritic cells are phagocytic. Neutrophils are the first immune cells to enter the site of inflammation and play an important role in acute phase response (52, 53). Macrophages are the most efficient phagocytes. Macrophages also perform antigen-presenting functions and secrete cytokines, which modulate immune responses. There are two subsets of macrophages - classically activated and alternatively activated macrophages, which vary in their receptor expression and functions (57). NK cells can recognize virally infected cells and tumor cells by signals such as lower MHC I expression, stress protein or non-self ligand expression, and exert cytotoxic effects on the cells by secreting enzymes such as perforin and granzymes (52, 58). They also secrete cytokines that activate other immune cells (58). Dendritic cells are the principal antigen-presenting cells (APCs), and they act as a major link between innate and adaptive immune responses (52, 53, 59).

1.3.2. Adaptive immunity

Adaptive immunity is mediated through the specific recognition and elimination of immunogenic pathogens and transformed cells. Adaptive immune responses are not present at birth, and these responses are activated after the immune system encounters antigens. These responses are mediated via T and B cells. Adaptive immune responses are made possible by somatic gene rearrangements, which give T and B cells the extraordinary ability to interact with a wide variety of antigens through T cell receptors (TCR) and B cell receptors (BCR) or immunoglobulins (Igs). Memory response is a unique feature of the adaptive immune response, which helps it recognize and eliminate a previously encountered antigen with a faster and heightened immune response (52, 55). B lymphocytes or B cells perform effector functions by secreting antibodies, working as APCs, and secreting cytokines to

modulate the immune response. B cells develop in the bone marrow from lymphoid progenitors. They exhibit membrane-bound Igs, which serve as BCRs. B cells get activated in response to antigens in peripheral lymphoid organs, and they get converted into plasma cells or memory cells. Plasma cells are short-lived cells that secrete antibodies (Igs). Antibodies are the main mediators of humoral immunity. Antibodies prevent the pathogens from invading or coat the target cells for phagocytosis as well as complement-mediated killing. Memory cells are long-lived cells that produce heightened immune responses on re-encounter with the same antigen (52, 53, 55).

T lymphocytes or T cells originate from lymphoid progenitors in the bone marrow but complete most of their development in the thymus. All T cells express the T cell receptor. To be activated, naïve T cells need to encounter antigens and need their TCRs to recognize antigens presented in the context of MHC. In addition to the TCR-MHC interaction, the interaction of co-stimulatory molecules, CD28, ICOS, or CD40L on the surface of T cells with B7.1/B7.2 (CD80/CD86), ICOSL, or CD40 is necessary (52, 60). MHC class I molecules are expressed on all nucleated cells of the host, and they display peptides expressed endogenously in the cell. MHC class II molecules are expressed on the surface of APCs, and they express exogenous proteins which are endocytosed or phagocytosed by them. T lymphocytes are divided into two subtypes based on their functions and cell surface markers, CD4 and CD8. Cytotoxic T lymphocytes (T_C or CTLs) express CD8 and recognize antigens displayed on MHC I. Their main function is to recognize and exert cytotoxic actions on infected or transformed cells. T helper lymphocytes (T_H) express CD4 membrane glycoprotein, and they recognize antigens displayed on MHC II expressed on APCs, including macrophages, DCs, and B lymphocytes. They effect immune responses through the

secretion of specific cytokines. Due to varying activation signals, $CD4^+$ T cells can differentiate into different subsets such as T helper 1 (T_H1), T helper 2 (T_H2), T helper 9 (T_H9), T helper 17 (T_H17), T helper 22 (T_H22), follicular helper T cells (T_{FH}), and regulatory T cells (Tregs). T helper cells secrete cytokines which activate immune responses. Tregs regulate and suppress immune responses (52, 53, 55).

1.3.3. Immune responses in cancer

The immune system plays an important role in defending against cancer. This function can be particularly appreciated in immunocompromised individuals who are more susceptible to cancer compared to immunocompetent individuals (52, 59, 61). In the 1950s, Frank Burnet and Lewis Thomas formulated the ‘immune surveillance’ hypothesis according to which immune cells would target and destroy the tumor cells. Since then, it has been determined that the interaction between tumors and the immune system is complex and that this interaction can have antitumor as well as tumorigenic effects. The earlier hypothesis has now been modified to include three phases of tumor growth. The first phase is the elimination phase, in which immune cells recognize and destroy potential tumor cells. The second phase is the equilibrium phase, in which tumor cells undergo changes or mutations that favor their survival. The third phase is the immune escape phase, in which tumor cells have acquired the ability to evade the immune system and grow in an unimpeded manner (52, 62).

The immunogenicity of tumor cells arises from certain changes in their cell surface protein expression that differs from normal cells. Such changes include the production of novel proteins, which are not included in the repertoire of normal cells, called tumor-specific antigens (TSA). Changes may also be in the expression pattern

of certain proteins compared to normal cells, and such normal proteins with altered expression in tumor cells are called tumor-associated antigens (TAA) (52, 59).

Immune cells from both innate and adaptive immune systems contribute to the immune response against tumor cells. In general, the immune cells can be divided into two groups based on their functions in the tumor: antitumor immune cells and protumor immune cells, also termed immunosuppressive cells. Antitumor immune cells include CD8+ cytotoxic T cells, effector CD4+ T cells, natural killer (NK) cells, dendritic cells (DCs), and M1-polarized macrophages. Immunosuppressive cells include regulatory T cells (Tregs), myeloid-derived suppressor cells (MDSCs), and M2-polarized macrophages (63).

$CD8^+$ cytotoxic T cells or CTLs are the most powerful effector cells in the antitumor immune response. $CD8^+$ T cells can interact with antigens presented in the context of MHC class I molecules. In the TME, CTLs use two pathways for killing the cancer cells: Granule exocytosis and Fas ligand (FasL)-mediated apoptosis induction. In the granule exocytosis pathway, CTLs release perforin to create pores in the membrane of target cells and then release granzymes which penetrate the surface of target cells and mediate apoptosis via caspases. In the FasL pathway of apoptosis, CTLs through FasL activate the Fas death receptor on target cells which in turn activates the extrinsic apoptotic pathway. CTLs also secrete interferon-γ (IFNγ) and tumor necrosis factor α (TNFα) to induce cytotoxicity (59, 63, 64). The activation and regulation of CTLs require two signals: TCR and immune checkpoint signals. Immune checkpoints can be divided into two types – inhibitory checkpoints such as CTLA-4, PD-1 and stimulatory checkpoints such as ICOS, CD40L, CD27. Tumor cells can inhibit the activation of CTL by expressing PD-L1, which binds to PD-1 (63, 64).

In addition to CTLs, NK cells can also induce cytotoxicity of cancer cells. NK cells can recognize tumor cells that are deficient in major histocompatibility complex (MHC) class I molecules (missing self) using killer-cell immunoglobulin-like receptors (KIRs). NK cells also recognize tumor cells that have upregulated stress ligands using NKG2D receptors (induced self) or tumor cells that are opsonized with antibodies specific for tumor antigens. After recognition, NK cells mediate cytotoxicity through the release of perforin and granzymes to induce apoptosis of the tumor cells. NK cells secrete cytokines such as IFNγ, IL-10, TNFα, GM-CSF, CCL3, CCL4, CCL5, which recruit other immune cells. NK cells effect an early and potent production of IFNγ, which in turn causes induction of MHC class II molecules on APCs, activation of myeloid cells, and induction of T helper 1 (T_H1) cells (59, 63, 65).

Dendritic cells (DCs) are the most potent APCs. DCs get activated or matured by DAMPs or type I interferons released in the TME. Mature DCs, which express CCR7, migrate to the lymph node, cross-present antigens, and prime CTLs using MHC and co-stimulatory molecules. CTLs which get activated migrate to TME to cause cytotoxic effects. DCs can also support T_H1 cell polarization of CD4+ T cells. In addition to antigen presentation, DCs secrete cytokines such as IL-12 and type I interferons. IL-12 helps in T_H1 cell and $CD8^+$ T cell priming (63, 66-68).

Of the different subtypes of $CD4^+$ T helper cells that exert antitumor effects, T_H1 is the most potent. $CD4^+$ T helper cells mediate the induction and clonal expansion of $CD8^+$ T cells via CD40–CD154 interaction and IL-2 production. $CD4^+$ T cells can help in the activation and licensing of DCs to activate $CD8^+$ T cells. These responses help in the augmentation of antitumor immunity. $CD4^+$ T cells can help in the conversion of $CD8^+$ T cells into memory CTLs. Besides IL-2, $CD4^+$ T cells secrete IFNγ and TNFα.

$CD4^+$ T cells with cytotoxic effects called $CD4^+$ CTL have been identified, and they identify antigens via MHC class II molecules (63, 69, 70).

M0 macrophages are highly plastic and can differentiate into M1 or M2 macrophages based on the cytokine signals (71). M1-like macrophages, also called classically activated macrophages, are stimulated by the type 1 cytokines such as IFNγ and TNFα (72). They can effect antitumor response by performing as APCs in the context of MHC II. They enhance the differentiation of naïve CD4+ cells and produce chemokines and cytokines to recruit and activate cytotoxic $CD8^+$ T cells and NK cells (72). M2-like macrophages, also called alternatively activated macrophages, are stimulated by type 2 cytokines such as IL-4, IL-10, and IL-13 (63, 72). Most tumor-associated macrophages (TAMs) exhibit M2-like phenotype with protumor characteristics (71, 72). TAMs inhibit T cell cytotoxicity through depletion of l-arginine via the release of arginase 1 or depletion of tryptophan by indoleamine 2,3-dioxygenase (IDO). TAMs secrete chemokines such as CCL5, CCL22, and CCL20, which recruit Tregs, and cytokines such as IL-10 and TGF-β, which induce Tregs. TAMs secrete vascular endothelial growth factor A (VEGFA) and angiogenic CXC chemokines (CXCL8 and CXCL12), which increase angiogenesis. TAMs facilitate metastasis by producing cathepsins and matrix-remodeling enzymes (72-75). Though conventionally classified as M1 and M2, recent studies have suggested that this classification is an oversimplification as TAMs identified in TME exhibit qualities of both M1 ($NOS2^+$) and M2 ($Arg1^+$) macrophages. Suggestions have been made to describe macrophages using multiple markers and well-defined model systems to avoid ambiguity (74).

Tregs are a subset of CD4+ T cells that express CD4, CD25, and the transcription factor, FoxP3 (Forkhead box P3). Tregs are classified into two subsets according to their site of development. Natural Tregs (nTregs) develop in the thymus while induced Tregs (iTregs) develop from conventional, naive T cells in the periphery in response to TCR stimulation with retinoic acid or TGF-β. Tregs are highly immunosuppressive in function and promote immune tolerance in normal individuals. In the tumors, Tregs produce immunosuppression through a variety of mechanisms. Tregs constitutively express CTLA-4, which can interact with CD80 or CD86 on APCs and suppress their ability to activate T cells. They express IL-2R, which acts as a sink for IL-2 to deplete the cytokine in the TME. Tregs interact with effector T cells using checkpoint molecules which inhibit the latter's functions (76-78).

MDSCs are potent immunosuppressive cells. They are a heterogeneous group of immature myeloid cells (79). The population of MDSCs gets expanded in chronic inflammatory conditions such as cancer due to cytokines such as VEGF, G-CSF, GM-CSF, IFNγ, prostaglandins, TGF-β, IL-6, and IL-10 (80). In mice, MDSCs are characterized by the expression of CD11b and Gr-1. (79). There are two subtypes of MDSC – monocytic MDSC (M-MDSC or mMDSC) and granulocytic or polymorphonuclear MDSC (G-MDSC or gMDSC or PMN-MDSC). In mice, mMDSC is characterized as $CD11b^{+}/Ly6G^{-}/Ly6C^{hi}$, and gMDSC is characterized as $CD11b^{+}/Ly6G^{+}/Ly6C^{lo}$ (79). mMDSCs can get further differentiated into TAMs, whereas gMDSCs are fully differentiated (80, 81). MDSC subtypes differ in their mechanisms of immunosuppression as well as potency to cause immunosuppression (80). MDSC, through the activity of arginase, increases the catabolism of L-arginine and depletes its levels in the TME. L-arginine shortage inhibits T cell proliferation (80, 82). MDSCs generate oxidative stress by increasing levels of reactive oxygen species

(ROS) and inducible nitric oxide synthase (iNOS). ROS and iNOS cause the production of reactive nitrogen species such as nitric oxide (NO) and peroxynitrite. NO suppresses T cell function via inducing T cell apoptosis or via the nitration and desensitization of TCR (80, 82). Peroxynitrites are highly reactive oxidizing agents which can induce posttranslational modification of proteins by nitrating tyrosine residues. This can make T cells unresponsive in the TME (80, 83). gMDSCs express high levels of ROS and low levels of NO, whereas mMDSCs express low levels of ROS and high levels of NO. Arg-1 is expressed in both (80). MDSCs express the enzyme indoleamine 2,3-dioxygenase (IDO), the first and rate-limiting enzyme of tryptophan catabolism via the kynurenine pathway, which results in the depletion of tryptophan, an amino acid essential for T cell activation, and this causes decreased T cell proliferation (82). MDSCs activate Tregs through the production of TGF-β and IL-10, and Tregs can potentiate immunosuppression (82, 84).

1.3.4. Prognostic role of immune cells in breast cancer

Immune cell infiltrations in the tumor correlate with factors such as survival, response to treatment, or recurrence, and therefore can serve as prognostic indicators in breast cancer. In breast cancer, it has been observed that the prognostic significance of immune cell infiltration can differ between various subtypes (85, 86). Triple-negative breast cancer (TNBC) has been reported to have a greater prevalence of increased immune cell infiltrates in the tumor compared to other breast cancer subtypes. The immunogenicity of TNBC could be attributed to increased genetic mutations, which lead to more aberrant protein expression, which may be recognized by the immune system (87).

The presence of $CD8^+$ T cells in TME is associated with a significant reduction in the mortality risk from breast cancer in ER-negative and ER-positive HER2-positive subtypes (86). Studies have found higher rates of pathological complete response (pCR) in cancers with higher levels of $CD8^+$ T cell infiltration after neoadjuvant chemotherapy (86, 88). In basal type of breast cancer (TNBC), it was found that total $CD8^+$ counts were associated with better breast cancer specific survival (89).

Among $CD4^+$ T cells, T_{FH} has been linked to better survival and response to chemotherapy in breast cancer (90). The link between $CD4^+$ T cells with TNBC outcomes has not been elucidated yet (85).

Inhibitory checkpoint molecule PD-L1, which binds to T cells and causes their inactivation, is commonly expressed in TNBC (85, 86). In addition to tumor cells, PD-L1 could be expressed in the breast stroma (85, 91). Regarding the association of PD-L1 with prognostic outcomes, conflicting results have been obtained (91). Some studies have predicted better disease-free survival (92), relapse-free survival (93) with PD-L1 expression, and increased overall survival in PD-L1-positive TIL-high cancers (94). On the contrary, other studies have predicted a worse overall survival with PD-L1 expression (95). Potential sources of inconsistencies in the literature include differences in methodology of PD-L1 measurement – gene expression vs. protein expression, usage of different antibody clones, lack of standardized methods of evaluating PD-L1 measurement, heterogeneity in samples, or stromal expression of PD-L1. Limitation in the number of studies and smaller sample size of studies make it difficult to assess the prognostic value of PD-L1 unambiguously, and more studies are needed to understand the prognostic importance of PD-L1 in breast cancer.

Nevertheless, high expression of PD-L1 is associated with a better response to PD-L1 therapy (85, 86).

Tregs have been associated with high grade and ER-negative breast cancers (86). They have been particularly found to be enriched in TNBC patients compared to other types (85). Traditionally, Tregs have been associated with immune suppression and poor outcomes. But recent data in TNBC indicate that a higher Treg density is associated with better prognostic outcomes (96, 97). It is yet unclear why Tregs are associated with a favorable prognosis. Further studies are needed to understand whether there is a mechanistic role of Tregs in this regard.

In clinical studies, NK cells are characterized using the markers CD16 and CD56 along with CD3 in the case of NKT cells (54, 98). From a retrospective study of 14 breast cancer patients, markers of NK activation were associated with increased relapse-free survival (99). Studies have not yet been undertaken to analyze NK cells in different breast cancer subtypes.

Clinically, macrophages are identified using CD68 as a pan-macrophage marker and CD163 as a marker specific for M2. In breast cancer patients, CD68 and CD163 are associated with poor outcomes (86, 98). Specific breast cancer subtypes may interact differently with macrophages. Data from *in vitro* co-culture studies show that lesser differentiated tumors such as TNBC tend to differentiate macrophages towards the more suppressive M2 phenotype, whereas more differentiated tumors tend to differentiate macrophages towards the M1 phenotype (86). In breast cancer patients, a greater prevalence of M2 macrophages is seen in the TNBC subtype than the HER2+ subtype (85).

In humans, a common MDSC marker has not been determined yet (100). MDSC subtypes can be characterized as $CD11b^{+}/CD14^{-}/CD15^{+}$ for gMDSCs and $HLA\text{-}DR^{-/lo}/CD11b^{+}/CD14^{+}/CD15^{-}$ for mMDSCs (100, 101). Circulating MDSCs have been found to be elevated in breast cancer patients, and the numbers positively correlate with clinical cancer stage and metastatic burden (85, 102). A very few clinical studies have been undertaken pertaining to MDSC in breast cancer, and the prevalence and significance of MDSC in TNBC are not known yet.

1.4. MOUSE MODELS OF BREAST CANCER

Preclinical models which recapitulate the human breast cancer phenotype could serve as great experimental tools for mechanistic studies in breast cancer to understand tumor biology as well as to design therapeutics. Many mouse models have been used as preclinical models of breast cancer with considerable success. Mouse models of breast cancer that are used to study metastasis can be broadly classified into two categories – genetically engineered models and transplantable models (103-105). Genetically engineered models are a great tool to understand spontaneous tumor initiation and metastatic progression. However, these tumor models are associated with drawbacks such as heterogeneity in tumors due to the usage of different strains of mice and taking a longer duration to achieve metastasis (103, 104).

Transplantable models involve the intravenous, intraperitoneal, subcutaneous, or orthotopic inoculation of cancer cells or tissues into mice (103). Transplantable models of breast cancer can be classified into xenograft models or syngeneic models based on the origin of the breast cancer cell (104, 105). Xenografts transplanted for breast cancer studies include tissues or human cancer cell lines derived from breast

cancer patients (104, 105). Xenografts are usually grown in mice that are immunocompromised. Xenograft tumor models have significant disadvantages. Since the host mice in a xenograft model should be immunocompromised, it precludes the study of host immune response against the tumors (104). Immunodeficient mice have been observed with phenotypical changes such as altered blood vessel formation, which might influence the metastatic process (104, 106). Further, the cancer cell-stromal cell interactions do not optimally occur in xenografts due to cross-species boundaries, which could be another impediment to cancer studies (104).

Syngeneic transplantable models are tumor cell lines derived from spontaneous tumors or carcinogen-induced tumors in inbred mice which possess similar genetic background as the host mice. Advantages of syngeneic models are that the implanted tumor cells and host cells are of a similar genetic background which enables tumor-host interactions and that these models are compatible with immunocompetent mice (104). Orthotopic inoculation of tumor cells causes induction of spontaneous metastasis, which closely resembles human metastatic development (104, 107). Among the syngeneic mammary tumor models, 4T1 and its derivates are the most commonly used (107).

1.4.1. 4T1.2 tumor model

4T1 tumor cell line was derived from a spontaneous tumor that arose in a BALB/c mouse (108). 4T1.2 was derived from single cell cloning of 4T1 as a cell line that is capable of being highly metastatic and preferentially metastasizes to bone (109). 4T1.2 has a TNBC phenotype and resembles human basal-like breast cancer (110). The metastatic property of the 4T1.2 model makes it a model that mimics stage IV breast cancer. Further, 4T1.2 metastasizes to clinically relevant sites such as bone,

lung, lymph node, and spine, which resembles the clinical course of late-stage breast cancer (111). Because of these characteristic features, the 4T1.2 mammary tumor model is a good experimental system for studying metastatic triple negative breast cancer. However, this model does not possess any known tumor antigen. This feature does not recapitulate the human TNBC phenotype, which expresses many tumor antigens and is highly immunogenic (87). Because of the lack of identifiable tumor antigens in the 4T1.2 cells, the tumor model has limited immunogenicity, and it precludes the analysis of antigen-specific immune responses, which is an important aspect of antitumor response. This feature poses a major limitation to use this model in immunologic studies pertaining to breast cancer.

1.4.2. 4T1.2-HER2 tumor model

Modification of tumor cell lines to express tumor antigens is a strategy to increase the immunogenicity of tumor models (112, 113). To make the 4T1.2 cell line more immunogenic, the 4T1.2 cell line was transduced with a retroviral vector which contained the cDNA for HER2 (human erbB-2) (114). Preliminary studies were undertaken to understand the *in vitro* and *in vivo* tumor growth characteristics and immune responses in the early phase of tumor growth (115).

In vitro, the tumor growth characteristics of the 4T1.2-HER2 cell line were similar to the parental cell line, 4T1.2. However, the *in vivo* growth characteristics differed significantly between 4T1.2 and 4T1.2-HER2. Tumor growth of 4T1.2 tumors ($5x10^4$ cells inoculated) progressed rapidly (data not shown), and the mice became moribund at day 30. Tumor growth of 4T1.2-HER2 did not show a rapid linear increase like the 4T1.2 tumors but had a pattern that consisted of three phases: (i) initial tumor growth, (ii) spontaneous tumor regression, and (iii) a second phase of tumor outgrowth

or complete tumor rejection (**Fig. 1.1A**). To assess whether adaptive immunity could be involved in mediating the tumor regression, 4T1.2-HER2 cells were inoculated into immunodeficient BALB/c *scid* mice. In these mice, 4T1.2-HER2 tumor growth progressed rapidly without regression which supported the role of adaptive immune response in mediating tumor regression in wild type mice (**Fig. 1.1B**).

The immune response from the initial phase of tumor growth showed that tumor growth was associated with the accumulation of immune suppressive MDSCs, and tumor regression was associated with CD4 and CD8 T cells (**Fig. 1.2**). Further, antigen-specific IFNγ secretion against HER2 was observed in the early phases, supporting the premise that HER2 is being used as a tumor antigen in this model (115).

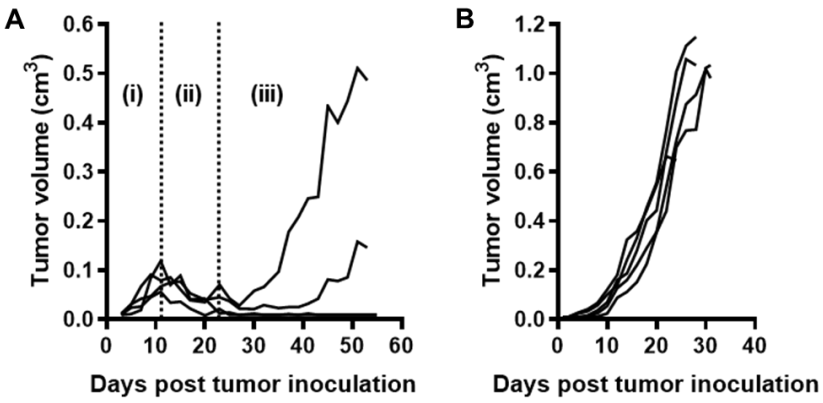

Figure 1.1. *In vivo* tumor growth of 4T1.2-HER2 tumor cells in BALB/c wildtype and BALB/c *scid* mice. *In vivo* tumor growth of individual mice **(A-B)**. 4T1.2-HER2 ($5x10^5$ cells inoculated) tumor growth in wildtype BALB/c mice (n=4) **(A)** consisted of three phases: (i) initial tumor growth, (ii) spontaneous tumor regression, and (iii) a second phase of tumor outgrowth or complete tumor rejection. **(B)** In immunodeficient BALB/c *scid* mice (n=5), 4T1.2-HER2 tumor ($5x10^5$ cells inoculated) demonstrated a rapid progression with no spontaneous regression phase (115).

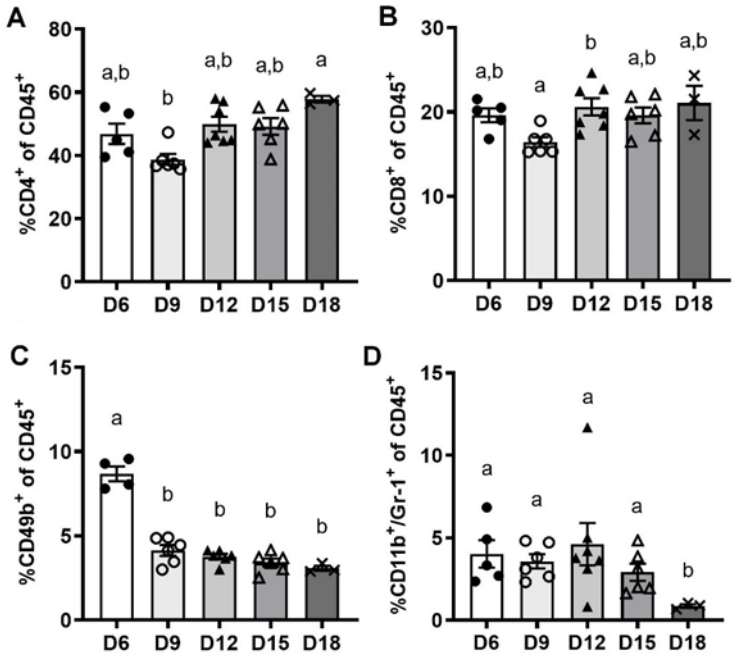

Figure 1.2. Tumor-infiltrating effector cells and immunosuppressive cells during 4T1.2-HER2 initial tumor growth and regression. The percentage of tumor-infiltrating $CD4^+$ **(A)** (Kruskal-Wallis test, KW=14.35, p=0.006) and $CD8^+$ **(B)** (one-way ANOVA, F(4,22)=3.35, p=0.028) T cells was reduced from D6 to D9 and increased after D9. The percentage of tumor-infiltrating $CD49b^+$ cells **(C)** (one-way ANOVA, F(4,20)=55.01, p<0.001) was reduced at D9-18 compared to D6. The percentage of tumor-infiltrating $Gr\text{-}1^+/CD11b^+$ cells **(D)** (one-way ANOVA, F(4,22)=4.962, p=0.005) was reduced at D18 (115).

1.5. RATIONALE FOR CURRENT STUDY

In the preliminary studies of the 4T1.2-HER2 tumor model, a three-phased tumor growth pattern was seen with initial phases of tumor growth followed by regression and a third phase of varied tumor outcomes with rejection in some mice and outgrowth in some mice. However, no study has to date been undertaken to characterize the late phase of tumor growth during which some mice develop tumors, and some mice reject tumors. It remains to be understood if immune responses are involved in mediating the differences in tumor growth in the third phase. This study was undertaken to characterize the tumor growth, immune responses, and lung metastasis in the late stages of the 4T1.2-HER2 tumor model. Findings from this study would further our understanding of this murine mammary tumor model and help us to validate this model for intervention studies pertaining to breast cancer in pre-clinical settings.

1.6. AIMS AND HYPOTHESES

The objective of this study was to characterize tumor growth, immune outcomes, and metastatic burden in the late stages of tumor growth in the 4T1.2-HER2 murine mammary tumor model.

The overarching hypothesis is that increased primary tumor growth will be positively associated with the suppression of antitumor immune responses and greater metastatic burden in the 4T1.2-HER2 murine mammary tumor model.

Aim 1. Determine if tumor volume is associated with immune cell infiltration.

Hypothesis 1. Larger tumor volume at sacrifice will be negatively associated with antitumor immune cell infiltration and positively associated with immunosuppressive cell infiltration, and smaller tumor volume at sacrifice will

be positively associated with antitumor immune cell infiltration and negatively associated with immunosuppressive cell infiltration.

Aim 2. Determine if tumor volume is associated with antigen-specific IFNγ secretion.

Hypothesis 1. Smaller tumor volume at sacrifice will be associated with increased HER2-specific IFNγ secretion, and larger tumor volume at sacrifice will be associated with decreased HER2-specific IFNγ secretion.

Aim 3. Determine if tumor volume is associated with metastatic burden in the lungs.

Hypothesis 1. Larger tumor volume at sacrifice will be associated with increased metastatic burden, and smaller tumor volume at sacrifice will be associated with decreased metastatic burden.

CHAPTER 2: CHARACTERIZATION OF TUMOR GROWTH, IMMUNE AND METASTATIC OUTCOMES IN THE 4T1.2-HER2 TUMOR MODEL

2.1. INTRODUCTION

Breast cancer is the leading cause of cancer-related death in women worldwide (6, 7). Metastasis is the main cause of mortality in breast cancer (6). Clinically relevant mouse models can serve as study systems for mechanistic studies pertaining to tumor biology, immune responses, and therapeutic interventions in metastatic breast cancer. The murine triple-negative breast cancer (TNBC) model, 4T1.2, does not possess any tumor antigens, which limits the use of this model for studying immune responses. In order to increase the immunogenicity of the 4T1.2 cell line, a surrogate tumor antigen, HER2, was introduced, and this tumor cell line is called 4T1.2-HER2 (114).

We have previously demonstrated that *in vivo* growth characteristics of the 4T1.2-HER2 cell line are significantly different compared to the parental 4T1.2 cell line (115). The parental 4T1.2 tumors exhibit a rapid, continuous growth, whereas 4T1.2-HER2 tumors exhibit a three-phased growth pattern with a short period of initial tumor growth followed by spontaneous tumor regression and a third phase of heterogeneous tumor growth with some mice showing increased tumor growth while some mice rejected tumors (115). The adaptive immune response may mediate the regression of tumor in the early phase of 4T1.2-HER2 tumor model. Antigen specific immune responses against HER2 are observed in the tumors (115). Further, in both spleen and tumors during the early phase of tumor growth, the percentages of $CD4^+$ and $CD8^+$ T cells are associated with the tumor regression and the percentage of MDSC is associated with increased tumor growth (115).

In the experiments from the early phase of tumor growth, antitumor and HER2-specific immune responses were associated with tumor regression. However, the relationship between antigen specific immune response and the control of tumor growth in the third or later phase of tumor growth is not known. It is yet to be understood what drives tumor regression in some mice and what induces relapse of tumors in others. Thus, the goal of the current study is to evaluate whether the primary tumor growth heterogeneity seen in the late phase of tumor growth will be associated with immune responses in the 4T1.2-HER2 murine mammary tumor model.

2.2. MATERIALS AND METHODS

2.2.1. Tumor cell line and cell culture

4T1.2-HER2 or 4T1.2-erbB-2 is a murine metastatic breast cancer line. The cells were provided by Dr. Phillip Darcy (Peter MacCallum Cancer Centre, East Melbourne, Victoria, Australia). 4T1.2-HER2 cell line was generated by transducing 4T1.2 cells with a retroviral vector, Murine Stem Cell Vector (MSCV), encoding the cDNA for human HER2 or erbB-2 (114). The parental 4T1.2 cell line was derived from a spontaneous mammary tumor that arose in BALB/cfC3H mouse (108). The parental cell line is highly aggressive and spontaneously metastasizes to the lung, liver, lymph node, heart, bone, brain, and thoracic cavity (108, 109, 114, 116). 4T1.2-HER2 cells were cultured in Dulbecco's modified Eagle's medium (DMEM) (Life Technologies, Grand Island, NY) containing 10% fetal bovine serum (Gemini Bio-Products, Sacramento, CA), 2 mM L-glutamine (Mediatech, Manassas, VA), and 1% Penicillin-Streptomycin (Mediatech).

2.2.2. Animal model

Female BALB/c mice were obtained from Jackson Laboratory (Bar Harbor, Maine). The mice were 10-months old at the start of the study. The mice (n=60) were orthotopically injected with $2x10^6$ 4T1.2-HER2 cells in the fourth mammary fat pad of their left side. Primary tumor growth was measured three times/week using an electronic caliper. Tumor volume was calculated using the formula, tumor volume = ($short^2$ x long)/2. Mice were sacrificed at days 31, 35, 36, and 38 after tumor implantation. Mice were fed AIN-76A diet (Research Diets, New Brunswick, NJ) *ad libitum*. Mice were group housed in ventilated cages and maintained on a 12-hour light/dark cycle. All the mice were housed at the animal facility in Chandlee Laboratory, Pennsylvania State University. The Institutional Animal Care and Use Committee of the Pennsylvania State University approved all animal experiments.

2.2.3. Isolation of splenic and tumor-infiltrating immune cells

At sacrifice, spleens and tumors were harvested and single cell suspensions of splenocytes and tumor-infiltrating immune cells were prepared as previously described (43, 117). Spleens were isolated from individual mice, mechanically dissociated using a syringe plunger, and passed through a 70 µm nylon mesh strainer (BD Biosciences, Bedford, MA) to prepare a single cell suspension of splenocytes in RPMI complete medium (CM) containing RPMI 1640 (Mediatech) supplemented with 10% FBS (Gemini Bio-Products, Sacramento, CA), 0.1 mM non-essential amino acids (Mediatech), 1 mM sodium pyruvate (Mediatech), 2 mM glutamine (Mediatech), 10 mM HEPES (Mediatech), and 1% penicillin streptomycin (Mediatech). Primary tumors were isolated, weighed and minced into small pieces. Tumor pieces were incubated in RPMI medium with 0.03 mg/ml Liberase (Roche, Indianapolis, IN) and 12.5 U/ml

DNase I (Thermo Fisher Scientific, Waltham, MA) for 45 min at 37°C on a rotary sample mixer for digestion. Following this, the digested tumor was passed through a 70 µm nylon mesh strainer to prepare a single cell suspension of cells from the tumor. After mechanical disruption, both spleen and tumor samples were treated with ACK lysing buffer (Lonza, Basel, Switzerland), washed and resuspended in RPMI CM. Splenocyte counts and viability were analyzed via trypan blue (Mediatech) dye-based exclusion.

2.2.4. Flow cytometric analysis

Single cell suspensions of splenocytes and tumor-infiltrating immune cells were washed twice with flow buffer containing PBS (Mediatech) and 1% BSA (Rockland Immunochemicals, Limerick, PA). The cells were incubated sequentially with Fc block (BioLegend) for 10 min at 4°C, Zombie aqua viability die (BioLegend) for 15 min at 4°C, and then, they were stained with fluorescent dye-conjugated antibodies against extracellular markers (**Table 2.1**) or their corresponding isotype control antibodies for 30 min at 4°C. Following the incubation with antibodies, the cells were washed twice with flow buffer and fixed with BD Cytofix™ fixation buffer (BD Biosciences). In addition to the extracellular staining, intracellular staining was performed to analyze T regulatory cells using the Mouse Regulatory T Cell Staining Kit (eBioscience – Affymetrix, San Diego, CA) as per manufacturer's instructions. Briefly, after the extracellular staining of CD4 and CD25, cells were incubated in a fixation/permeabilization solution for 30 min, washed twice with permeabilization buffer, and stained with FoxP3 antibody (**Table 2.1**) or the corresponding isotype control antibody for 30 min. After the intracellular staining, cells were washed twice, and samples were analyzed using the flow cytometer within 12h. Flow cytometric

analysis was performed on BD LSR-Fortessa flow cytometer (BD Biosciences). The data obtained from the flow cytometer were analyzed using Flow Jo software (Tree Star, Ashland, OR). Using the Flow Jo software, single cells were first gated using forward vs. side scatter (FSC vs. SSC). Then, live cells were gated using Zombie aqua staining, and $CD45^+$ cells were selected using the pan-leucocyte marker, CD45. Following that, markers of myeloid, lymphoid, activation (tumors only), and memory cells were used to identify the specific immune cell subtypes.

Table 2.1. List of antibodies used in the flow cytometric analysis of immune cells.

Extracellular staining		
Antibody	**Clone**	**Vendor**
CD45	30-F11	BD
I-Ad	AMS-32.1	BD
CD11b	M1/70	BD
F4/80	BM8	BioLegend
CD11c	HL3	BD
Gr-1	RB6-8C5	BD
Ly-6C	AL-21	BD
Ly-6G	1A8	BD
CD4	RM4-5	BD
CD8	53-6.7	BD
CD49b	DX5	BD
CD25	PC61	BioLegend
CD69	H1.2F3	BD
CD44	IM7	BD
CD62L	MEL-14	BD
CD127	SB/199	BD
KLRG1	2F1	BD
CD279 (PD-1)	J43	BD
Intracellular staining		
Antibody	**Clone**	**Vendor**
FoxP3	FJK-16s	eBioscience

2.2.5. Antigen-specific IFNγ secretion

2.2.5.1. Antigen-specific IFNγ secretion from splenocytes

Splenocytes at a concentration of $25x10^6$ cells/flask were cultured in RPMI complete media with 10 µg/ml $HER2_{63-71}$ peptide (TYLPTNASL; CPC Scientific, San Jose, CA) in T25 flasks for 6 days to generate HER2 antigen-specific T cells. After 6 days, the cells were isolated and cultured in 24-well plates at a concentration of $1x10^6$ cells/well in CM along with irradiated splenocytes ($4x10^6$ cells/well; irradiated with 2000 Gy) from control mice and either 10 µg/ml HER2 p63-71 (TYLPTNASL; CPC Scientific), 10 µg/ml of influenza HA p518-526 peptide (IYSTVASSL; GenScript, Piscataway, NJ), 1 µg/ml anti-CD3 (BD Biosciences) or CM without any peptide. After 24 hours of incubation, supernatants were harvested and IFNγ was measured using ELISA MAX™ Deluxe Set (Biolegend, San Diego, CA), as per manufacturer's protocols. IFNγ was quantified with Epoch Microplate Spectrophotometer (Biotek, Winooski, VT). Each assay was performed in duplicate.

Prior to the main experiment, a pilot experiment was conducted to determine whether culture with irradiated 4T1.2-HER2 cells or HER2 peptide provided optimal conditions for the production of HER2-specific IFNγ response. For this experiment, splenocytes, from six mice that rejected tumors, were pooled and cultured using 4T1.2-HER2 cells or HER2 peptide to generate antigen specific T cell responses. In one experimental condition, at a concentration of $25x10^6$ cells/flask, splenocytes were cultured in RPMI CM with 10 µg/ml HER2 p63-71 (TYLPTNASL) peptide in T25 flasks for 6 days. In another experimental condition, splenocytes ($25x10^6$ cells/flask) were cultured with $1x10^6$ irradiated 4T1.2-HER2 cells (irradiation dose - 15000 Gy) in T25

flasks for 6 days. After 6 days, the cells from each flask were isolated and cultured in 24-well plates (Greiner Bio-One) at a concentration of $1x10^6$ cells/well along with $4x10^6$ irradiated splenocytes (irradiation dose - 2000 Gy). Splenocytes stimulated with HER2 peptides in bulk culture were restimulated with HER2 p63-71 peptide (TYLPTNASL; 10 ug/mL), influenza HA p518-526 peptide (IYSTVASSL; 10 ug/mL), anti-CD3 (1 µg/mL) or CM alone. Splenocytes stimulated with irradiated 4T1.2-HER2 cells in bulk culture were restimulated with $0.4x10^6$ irradiated 4T1.2-HER2 cells (15000 Gy), $0.4x10^6$ 4T1.2 irradiated cells (15000 Gy), anti-CD3 peptide (1 µg/mL) or CM alone. After 24 hours of incubation, supernatants were harvested and IFNγ was measured. Each assay was performed in duplicate.

2.2.5.2. Antigen-specific IFNγ secretion from TILs

Tumor cells ($1x10^6$ cells/well) were cultured in 24-well plates along with irradiated splenocytes ($4x10^6$ cells/well; irradiation dose - 2000 Gy) isolated from control mice, and HER2 p63-71 peptide (TYLPTNASL; 10 µg/ml), influenza HA p518-526 peptide (IYSTVASSL; 10 µg/ml), anti-CD3 (BD Biosciences) at 1 µg/ml as positive control, and CM alone. After 48 hours of incubation, supernatants were harvested and IFNγ was measured using ELISA MAX™ Deluxe Set (Biolegend), as per manufacturer instructions. IFNγ was quantified with Epoch Microplate Spectrophotometer (Biotek). Each assay was performed in duplicate.

2.2.6. Metastatic burden

Lungs were harvested at sacrifice and stored in RNA later (Life Technologies, Carlsbad, CA) at 4°C for 24 hours. After 24 hours, lungs were taken out of RNAlater

and stored at -80°C. Homogenization was done using QIAshredder homogenizer (Qiagen, Valencia, CA). mRNA was extracted using RNeasy Mini Kit (Qiagen) as per manufacturer's instructions. mRNA was quantified using Nanodrop ND-1000 spectrophotometer (Nanodrop Products, Wilmington, DE). RNA was reverse transcribed using the High-Capacity cDNA reverse transcription kit (Applied Biosystems, Foster City, CA) according to manufacturer's instructions. Metastatic burden was determined by quantifying the gene expression of gp70 using Taqman™ system (Applied Biosystems, Catalog# 4331182) on a Step-One Plus (Life Technologies, Carlsbad, CA) real time PCR instrument. Gene expression levels were reported using the Ct values representing the expression of the gp70 (gene of interest) and 18s (house-keeping gene), and ΔCt values denoting Ct(gp70)-Ct(18s).

2.2.7. Statistical analysis

All data were assessed for normality and equal variances, and either parametric or nonparametric analyses were used to detect differences between groups. If the data were skewed, log or square root transformation was done prior to statistical analyses. The association between spleen or tumor immune cells with tumor volume; the association between immune cell infiltration in the spleen and tumor; and the association between spleen and tumor immune cells with HER2-specific IFNγ response were calculated using Pearson's or Spearman's correlation analyses based on the distribution of data. Assessment of HER2-specific IFNγ response in the spleen and tumor was determined using Kruskal-Wallis test, followed by Dunn's multiple comparison test. Analysis of HER2-specific IFNγ responses in mice with high and low tumor volumes in the spleen and tumor were determined using 2-way ANOVA followed by Dunnett's multiple comparison test where appropriate; IFNγ data from the spleen

was skewed and was transformed (square root) prior to this analysis. To determine the linear relationship between lung metastasis and tumor volume, Mann-Whitney test was done. All analyses were conducted using GraphPad Prism 7 (GraphPad Software, San Diego, CA). All data are presented as mean ± SEM except mean tumor growth data which is presented as mean ± SD. Statistical significance was accepted at $p \leq 0.05$.

2.3. RESULTS

2.3.1. *In vivo* tumor growth

When 4T1.2-HER2 tumor cells ($2x10^6$ cells) were inoculated in the left fourth mammary fat pad of wildtype BALB/c mice, all the mice developed tumors. The mean tumor volume over time and the tumor growth curves of individual mice are shown in **Fig. 2.1**. The tumors exhibited a three-phase growth pattern – (i) initial phase of tumor growth (up to day 12 post-tumor implantation) (ii) an intermediate phase in which there was a mild growth regression (between day 12 and day 19 post-tumor implantation) (iii) a late phase of tumor growth where the mice experienced varied tumor growth responses (after day 20).

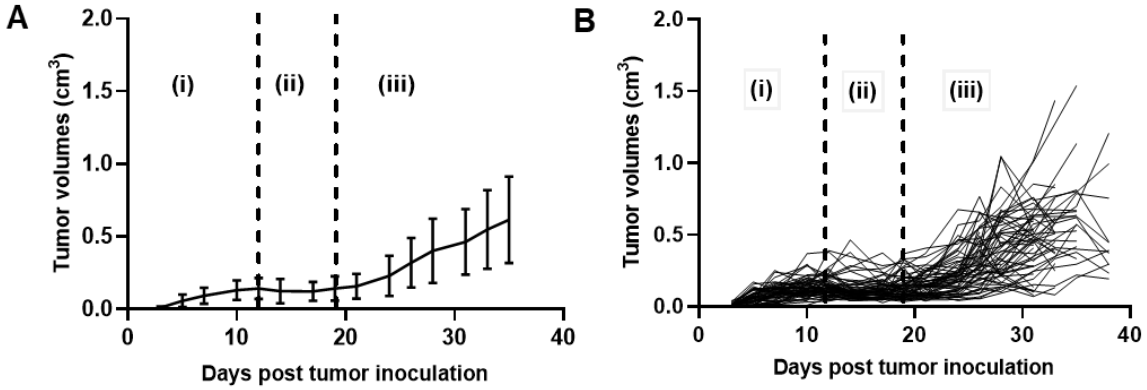

Figure 2.1. *In vivo* tumor growth characteristics of 4T1.2-HER2 tumor cells in BALB/c mice. 10-month-old female BALB/c mice (n=60) were orthotopically inoculated with $2x10^6$ 4T1.2-HER2 tumor cells. **(A)** The mean tumor volume ± SD over

time. **(B)** The tumor growth curves of individual mice. The tumor growth pattern can be divided into three phases – (i) an initial phase of tumor growth between day 0 to day 12; (ii) an intermediate phase in which there was either tumor growth cessation or mild tumor regression between day 10 to day 20; (iii) a late phase in which there was tumor growth after day 20.

2.3.2. Tumor growth comparison between the current study and other studies using the 4T1.2-HER2 tumor model

A comparison of tumor growth was made among different studies conducted in our lab using the 4T1.2-HER2 tumor model. In these studies, the mice used varied by their age and lab where the studies were conducted. Individual tumor growth curves of 5-month-old mice (n=32) (**Fig. 2.2A**), the current study using 10-month-old mice (n=60, only a few representative mice's tumor growth curves are shown in the figure) (**Fig. 2.2B**), 13-month-old mice (n=5) (**Fig. 2.2C**), and 17-month-old mice (n=9) (**Fig. 2.2D**) are shown. The mice from the current study were housed in the animal facility at Chandlee Laboratory and were group-housed, whereas the mice from all the other studies were housed in the animal facility at South Frear Laboratory and were singly housed. In the current study, when the tumor cells were inoculated in mice, tumor growth pattern was seen in three phases. While this three-phased tumor growth pattern was quite similar to the other studies, there were some notable differences. The average tumor volume of the mice in the current study was significantly increased compared to all the other studies. In the studies in which the mice were 5-months and 13-months-old, a sharp regression in tumor growth was observed between day 10 – day 20. In the present study, there was either a mild tumor growth regression or stagnation in the growth. In the 17-month-old mice, the second phase of tumor regression was less defined. During the third phase, tumor recurrence was seen only in 6/32 mice (18.75%) that were 5-months old (**Fig. 2.2A**). Tumor recurrence was seen

in all the mice (100%) that were 13-month-old, although the tumor growth remained very low in 3/5 mice, and the recurrence started only after day 38 (**Fig. 2.2C**). In the present study, none of the mice rejected tumors in the third phase of tumor growth. There was 100% recurrence and heterogeneity in tumor volumes was observed overall (**Fig. 2.2B**). In the mice that were 17-month-old, recurrence was seen in 7/9 mice (77.79%) (**Fig. 2.2D**). The overall survival for all the other studies was 40 days or greater, but in the current study, the mice became moribund around days 32-35. These findings suggest that age could be responsible for some of the changes observed. However, findings such as increased overall tumor volumes and a hastened tumor growth which led to poor survival in the current study maybe influenced by other factors such as housing conditions, lab environment, or loss of HER2 antigen.

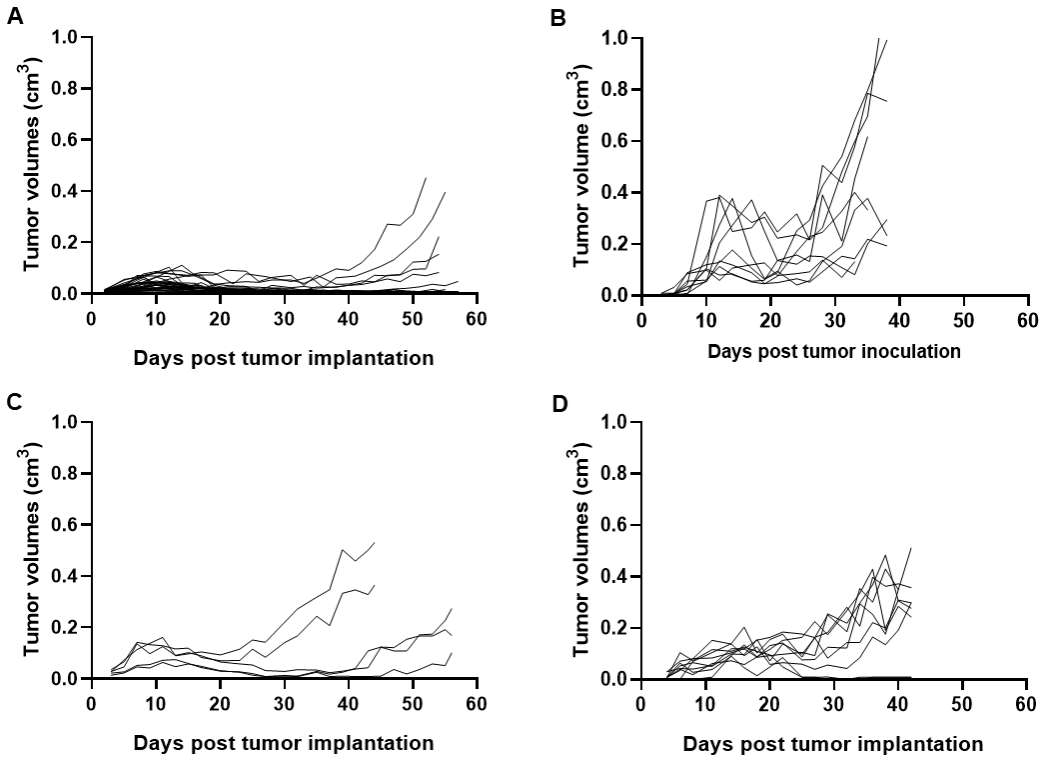

Figure 2.2. Comparison of tumor growths in different studies using the 4T1.2-HER2 tumor model. Individual tumor growth curves of 5-month-old mice **(A).** The representative individual tumor growth curves of 10-month-old mice in the current study **(B)**. Individual tumor growth curves of 13-month-old mice **(C)**. Individual tumor growth curves of 17-month-old mice **(D)**.

2.3.3. Number of splenocytes and tumor-infiltrating immune cells

Female BALB/c mice were sacrificed between days 31-38 post tumor implantation. The mean splenocyte count (± SEM) was 412.84x10^6 cells ± 49.24x10^6 cells (**Fig. 2.3A**). The mean count of immune cells in the tumor (± SEM) was 48.49x10^6 cells ± 6.94x10^6 cells (**Fig. 2.3B**).

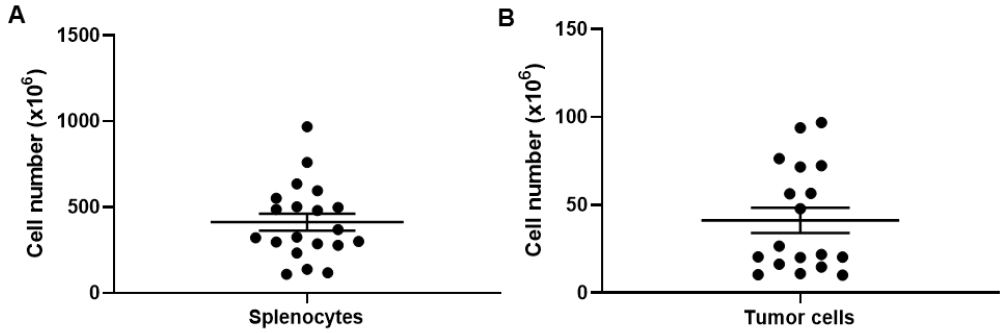

Figure 2.3. Number of cells in spleen and tumor. The number of splenocytes **(A)** and the number of immune cells in the tumor **(B)** at day 31-38 post tumor implantation.

2.3.4. Distribution of splenic myeloid and lymphoid cells

In the spleen, the percentage of $CD45^+$ cells that were antigen-presenting cells ($F4/80^+$ and $F4/80^+/CD11b^+$ macrophages, $I\text{-}Ad^+/CD11b^+$, and $I\text{-}Ad^+/CD11c^+$ dendritic cells), MDSCs ($Gr\text{-}1^+/CD11b^+$) and its subtypes, granulocytic or gMDSC ($CD11b^+/Ly6G^+/Ly6C^{lo}$) and monocytic or mMDSC ($CD11b^+/Ly6G^-/Ly6C^{hi}$), lymphoid effectors ($CD4^+$,$CD8^+$ T cells and $CD49^+$ NK cells) and regulatory T cells ($CD4^+/CD25^+/FoxP3^+$) are shown in **Fig. 2.4A**, **Fig. 2.4B**, and **Fig. 2.4C**, respectively. Immune cell ratios are shown in **Fig. 2.4.D**. All data are represented as mean ± SEM.

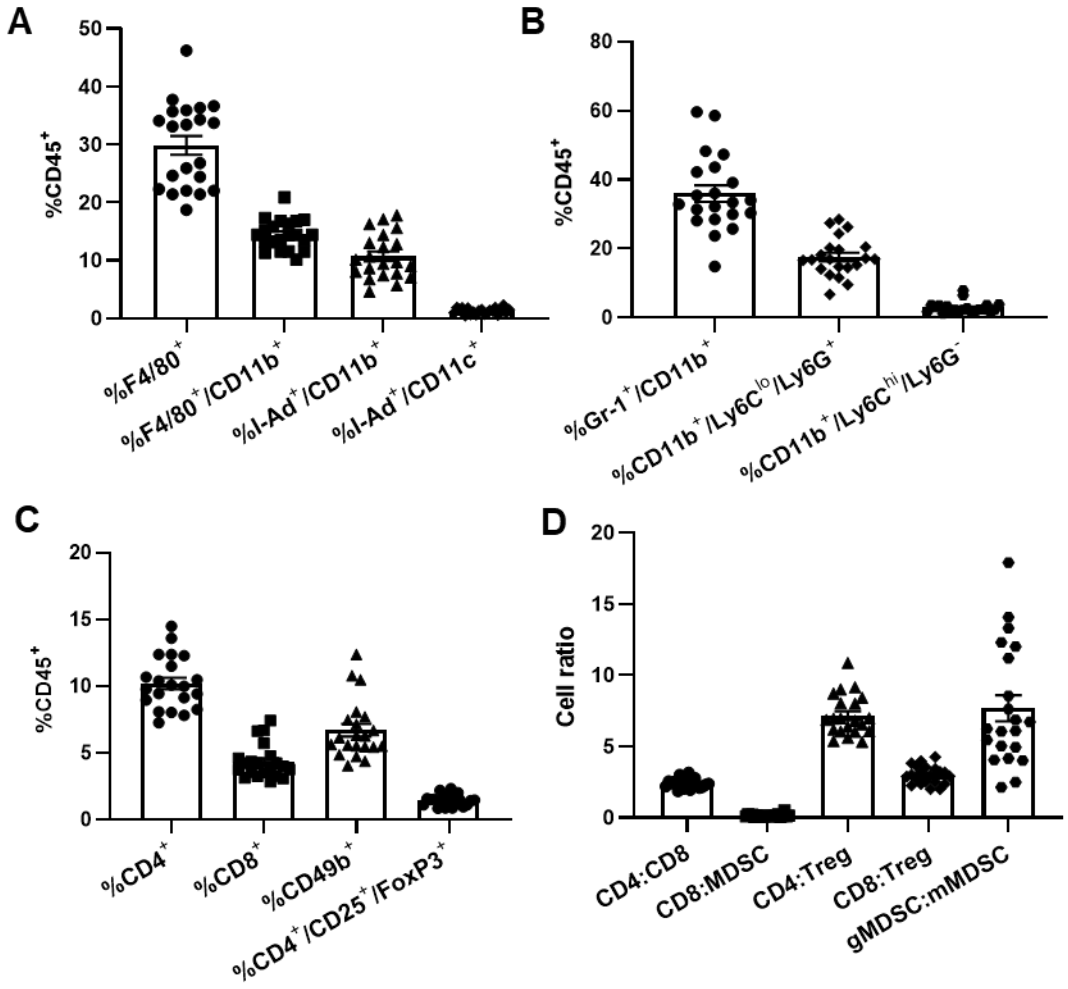

Figure 2.4. Immune cell distribution in the spleen. (A) Percentage of antigen-presenting cells **(B)** MDSC **(C)** Lymphoid effector and T regulatory cells and **(D)** Immune cell ratios at day 31-38 post tumor implantation. Data are presented as mean ± SEM.

2.3.5. Association between splenic myeloid and lymphoid cells and tumor volume

Among the myeloid cells of spleen, I-Ad$^+$/CD11b$^+$ (r=-0.492, p=0.0235, Pearson correlation) (**Fig. 2.5A**) and I-Ad$^+$/CD11c$^+$ dendritic cells (r=-0.653, p=0.0013, Pearson correlation) (**Fig. 2.5B**) were negatively correlated with tumor volume. Among the lymphoid cells, tumor volume was not correlated with CD4$^+$ T cells (r=-0.246, p=0.282, Pearson correlation) (**Fig. 2.5C**), CD8$^+$ T cells (r=-0.301, p=0.184, Spearman

correlation) (**Fig. 2.5D**) and NK cells (r=-0.294, p=0.196, Spearman correlation) (**Fig. 2.5E**). $CD4^+/CD25^+/FoxP3^+$ T regulatory cells were negatively correlated with tumor volume (r=-0.458, p=0.0366, Pearson correlation) (**Fig. 2.5F**). $Gr\text{-}1^+/CD11b^+$ MDSCs (r=0.598, p=0.0042, Pearson correlation) (**Fig. 2.5G**), and mMDSCs ($CD11b^+/Ly6C^{hi}/Ly6G^-$) (r=0.597, p=0.0055, Spearman correlation) (**Fig. 2.5H**) were positively associated with tumor volumes. In addition to this, the cell ratio of $CD4^+$:Treg was positively correlated with tumor volume (r=0.555, p=0.009, Pearson correlation) (**Fig. 2.5I**). The correlation analysis of all the splenic immune cell populations included in this study is provided in **Appendix A** (**Table 1**).

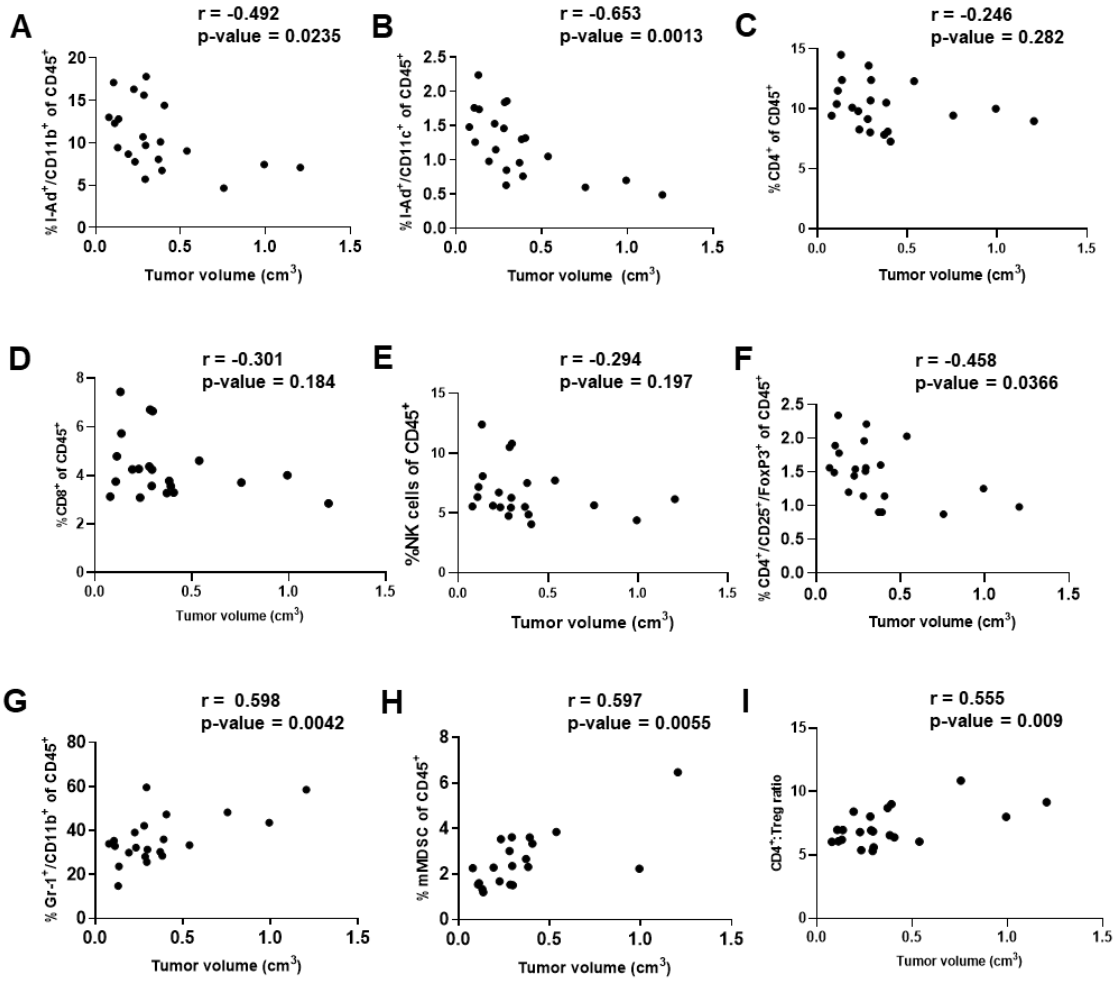

Figure 2.5. Association between immune cell populations in the spleen and final tumor volume. Tumor volume was negatively correlated with $I\text{-}Ad^+/CD11b^+$ cells **(A)** (r=-0.492, p=0.0235, Pearson correlation) and $I\text{-}Ad^+/CD11c^+$ dendritic cells **(B)** (r=-

0.653, p=0.0013, Pearson correlation). Tumor volume was not correlated with $CD4^+$ T cells **(C)** (r=-0.246, p=0.282, Pearson correlation), $CD8^+$ T cells **(D)** (r=-0.301, p=0.184, Spearman correlation) and NK cells **(E)** (r=-0.294, p=0.196, Spearman correlation). Tumor volume was negatively correlated with $CD4^+/CD25^+/FoxP3^+$ T regulatory cells **(F)** (r=-0.458, p=0.0366, Pearson correlation). Tumor volume was positively correlated with $Gr\text{-}1^+/CD11b^+$/MDSCs **(G)** (r=0.598, p=0.0042, Pearson correlation), $CD11b^+/Ly6C^{hi}/Ly6G^-$ mMDSC cells **(H)** (r=0.597, p=0.0055, Spearman correlation), and $CD4^+$:T regulatory cell ratio **(I)** (r=0.555, p=0.009, Pearson correlation).

2.3.6. Distribution of tumor-infiltrating myeloid and lymphoid cells

In the tumor, the percentage of $CD45^+$ cells that were antigen-presenting cells ($F4/80^+$ and $F4/80^+/CD11b^+$ macrophages, $I\text{-}Ad^+/CD11b^+$ and $Ad^+/CD11c^+$ dendritic cells), MDSCs ($Gr\text{-}1^+/CD11b^+$) and its subtypes, gMDSC ($CD11b^+/Ly6G^+/Ly6C^{lo}$) and mMDSC ($CD11b^+/Ly6G^-/Ly6C^{hi}$), lymphoid effectors ($CD4^+$,$CD8^+$ T cells and $CD49^+$ NK cells) and regulatory T cells ($CD4^+/CD25^+/FoxP3^+$) are shown in **Fig. 2.6A**, **Fig. 2.6B**, and **Fig. 2.6C**, respectively. Immune cell ratios are shown in **Fig. 2.6.D**. All data are represented as mean ± SEM.

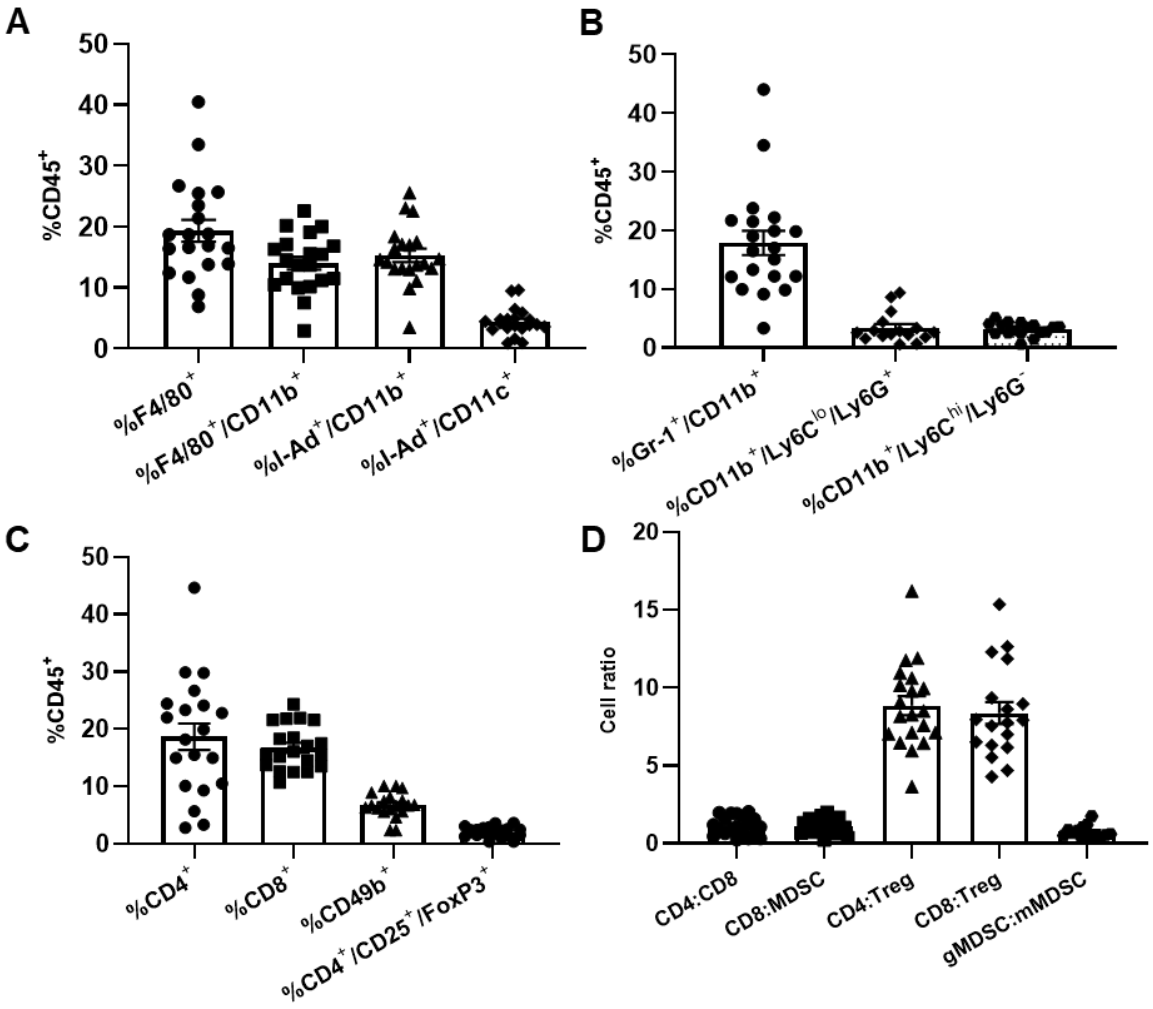

Figure 2.6. Immune infiltration in the tumors. (A) Percentage of antigen-presenting cells **(B)** MDSC **(C)** Lymphoid effector and T regulatory cells and **(D)** Immune cell ratios at day 31-38 post tumor implantation. Data are presented as mean ± SEM.

2.3.7. Association between tumor-infiltrating myeloid and lymphoid cells and tumor volume

Among the lymphoid cells, $CD4^+$ lymphocytes (r=-0.565, p=0.0094, Pearson correlation) (**Fig. 2.7A**), $CD49^+$ NK cells (r=-0.536, p=0.018, Pearson correlation) (**Fig. 2.7C**), and $CD4^+/CD25^+/FoxP3^+$ T regulatory cells (r=-0.661, p=0.0015, Pearson correlation) (**Fig. 2.7D**) were negatively correlated with tumor volume. $CD8^+$ lymphocyte (r=-0.363, p=0.1155, Pearson correlation) (**Fig. 2.7B**) was not correlated with tumor volume. $Gr\text{-}1^+/CD11b^+$ MDSC (r=0.556, p=0.0109, Spearman correlation)

(**Fig. 2.7E**) was positively associated with tumor volume. Among the cell ratios, ratio of $CD4^+$ to $CD8^+$ (r=-0.529, p=0.0165, Pearson correlation) (**Fig. 2.7F**), the ratio of $CD4^+$ to MDSCs (r=-0.623, p=0.0044, Pearson correlation) (**Fig. 2.7G**), and the ratio of $CD8^+$ to MDSCs (r=-0.612, p=0.0053, Pearson correlation) (**Fig. 2.7H**) were negatively correlated with tumor volumes. The correlation analysis of all the tumor immune cell populations included in this study is provided in **Appendix A** (**Table 2**).

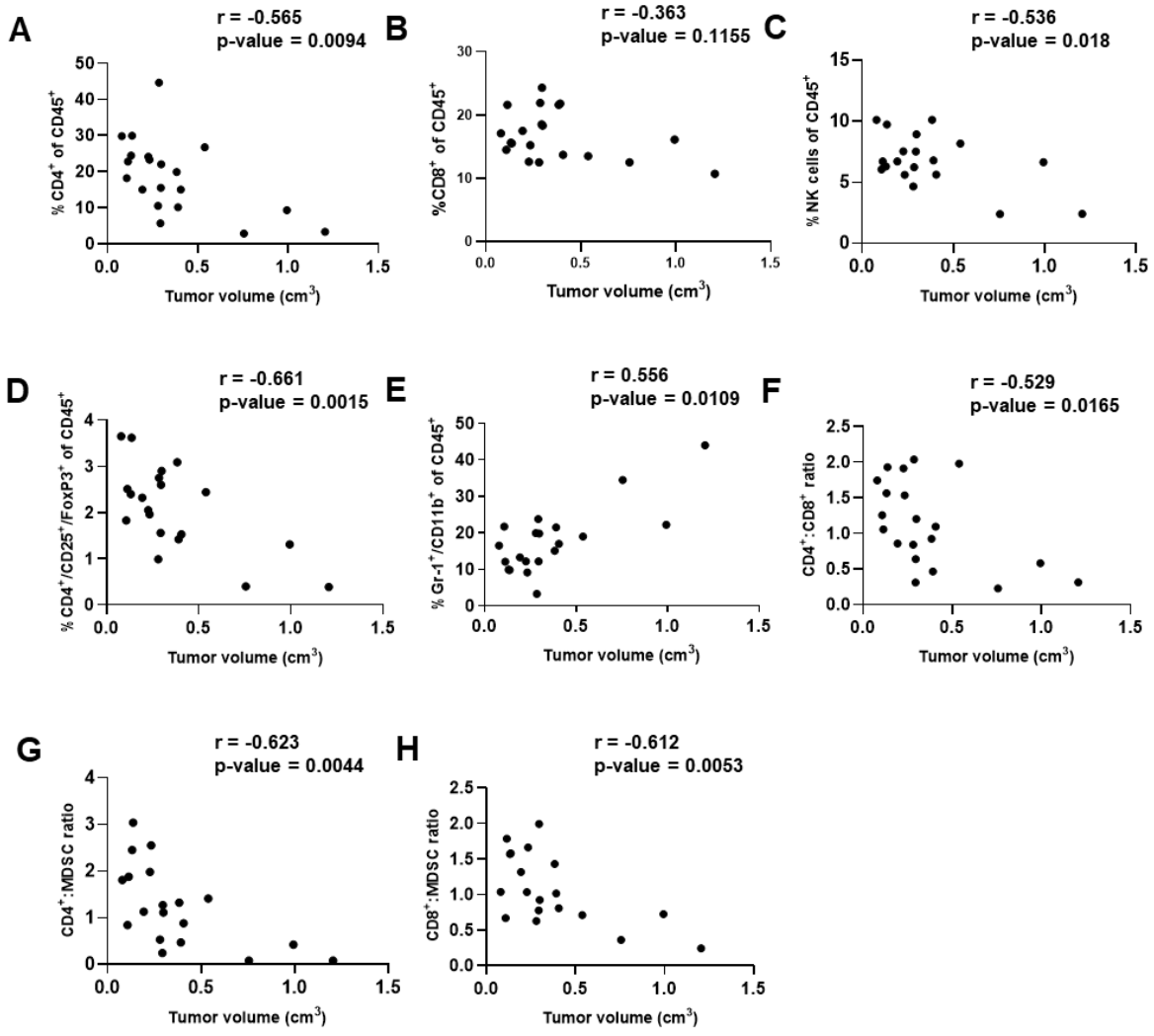

Figure 2.7. Association between immune cell infiltration in the tumor and final tumor volume. Tumor volume was negatively correlated with $CD4^+$ cells **(A)** (r=-0.565, p=0.0094, Pearson correlation), NK cells **(C)** (r=-0.536, p=0.018, Pearson correlation), and $CD4^+/CD25^+/FoxP3^+$ T regulatory cells **(D)** (r=-0.661, p=0.0015, Pearson correlation). Tumor volume was not associated with $CD8^+$ lymphocytes **(B)** (r=-0.363, p=0.1155, Pearson correlation). Tumor volume was positively associated with Gr-$1^+/CD11b^+$/MDSCs **(E)** (r=0.556, p=0.0109, Spearman correlation). Tumor volume

was negatively associated with the ratio of $CD4^+$ to $CD8^+$ **(F)** (r=-0.529, p=0.0165, Pearson correlation), the ratio of $CD4^+$ to MDSCs **(G)** (r=-0.623, p=0.0044, Pearson correlation), and the ratio of $CD8^+$ to MDSCs **(H)** (r=-0.612, p=0.0053, Pearson correlation).

2.3.8. Distribution of effector and memory cells in the tumor

In the tumor, distribution of naïve cells ($CD44^-/CD62L^+$), effector cells (EC) ($CD44^-/CD62L^-$) and memory cells - central memory cells (T_{CM}) ($CD44^+/CD62L^+$) and effector memory cells (T_{EM}) ($CD44^+/CD62L^-$) of $CD4^+$ and $CD8^+$ cell lineage are shown in (**Fig. 2.8A**). Effector cell subtypes – early effector cells (EEC) ($KLRG1^-/CD127^-$), memory precursor effector cells (MPEC) ($KLRG1^-/CD127^+$), short-lived effector cells (SLEC) ($KLRG1^+/CD127^-$) and double-positive effector cells (DPEC) ($KLRG1^+/CD127^+$) in $CD4^+$ and $CD8^+$ cell lineage are shown in (**Fig. 2.8B**). $CD69^+$ and PD-1^+ cells of the $CD4^+$ and $CD8^+$ lineage are shown in (**Fig. 2.8C**).

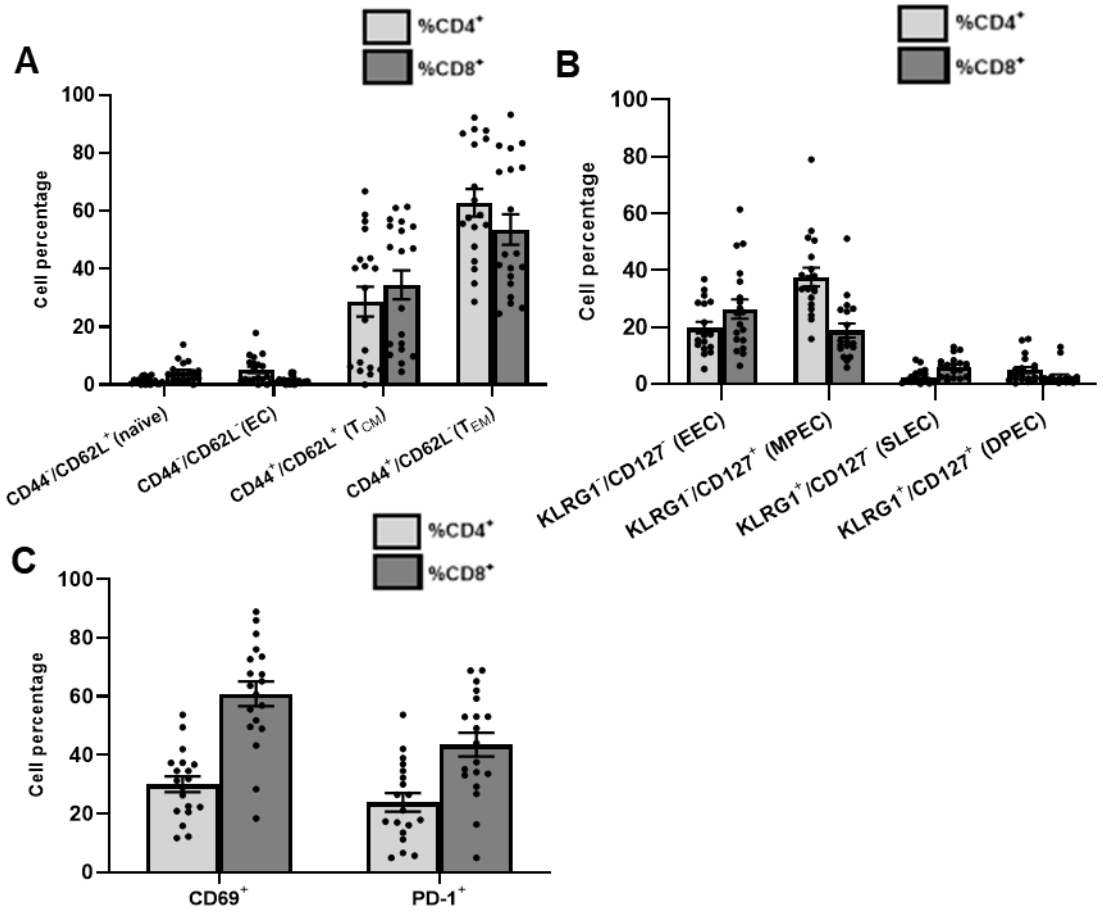

Figure 2.8. Effector and memory cell populations in the tumor. (A) Naïve cells, effector cells (EC) and memory cells - central memory cells (T_{CM}) and effector memory cells (T_{EM}) of $CD4^+$ and $CD8^+$ cell lineage. **(B)** Effector cell subtypes – early effector cells (EEC), memory precursor effector cells (MPEC), short-lived effector cells (SLEC) and double-positive effector cells (DPEC) in $CD4^+$ and $CD8^+$ cell lineage. **(C)** $CD69^+$ and PD-1^+ cells of the $CD4^+$ and $CD8^+$ lineage at day 31-38 post tumor implantation.

2.3.9. Association between tumor-infiltrating effector and memory cells and tumor volume

Central memory cells of both $CD4^+$ lineage (r=-0.6193, p=0.0047, Spearman correlation) (**Fig. 2.9A**) and $CD8^+$ lineage (r=-0.5386, p=0.0174, Spearman correlation) (**Fig. 2.9B**) were negatively correlated with tumor volumes. Tumor volume was positively correlated with effector memory cells of both $CD4^+$ (r=0.6724, p=0.0016, Pearson correlation) (**Fig. 2.9C**) and $CD8^+$ lineage (r=0.6263, p=0.0041, Spearman

correlation) (**Fig. 2.9D**). Tumor volume was positively associated with memory precursor effector cells (MPECs) of $CD4^+$ (r=0.7451, p=0.0003, Pearson correlation) (**Fig. 2.9E**) and $CD8^+$ lineages (r=0.5737, p=0.0102, Spearman correlation) (**Fig. 2.9F**). The correlation analysis of all the effector and memory cells included in this study is provided in **Appendix A** (**Table 3**).

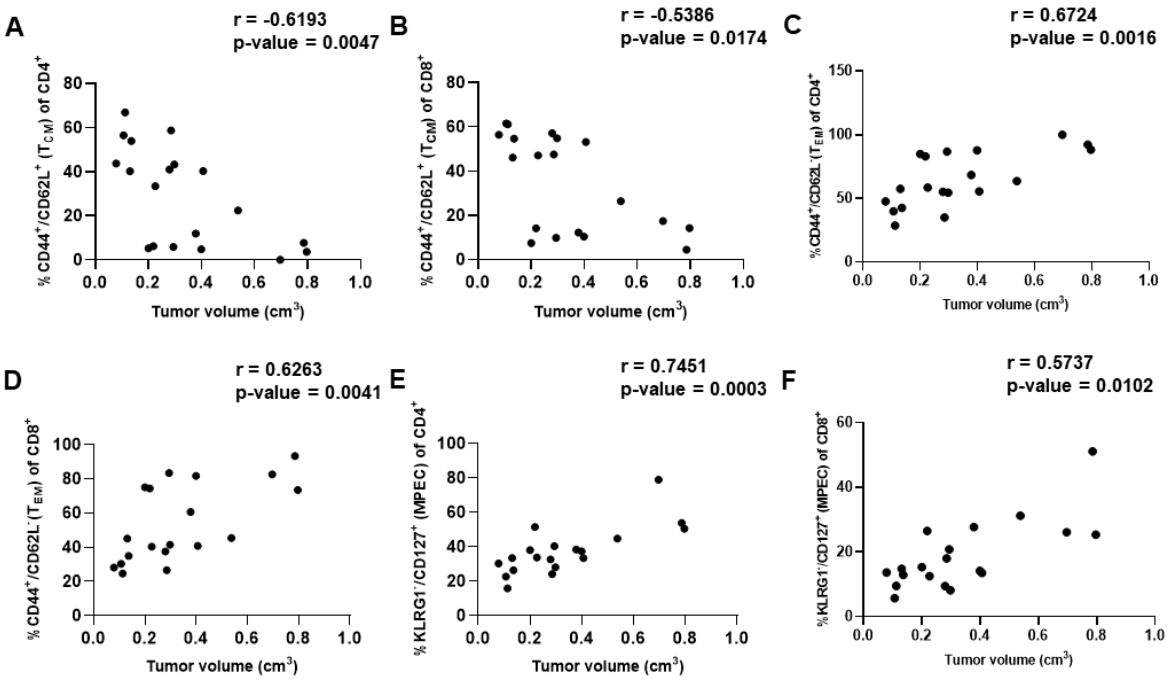

Figure 2.9. Association between effector and memory cells in the tumor and final tumor volume. Tumor volume was negatively correlated with central memory cells of $CD4^+$ lineage **(A)** (r=-0.6193, p=0.0047, Spearman correlation) and $CD8^+$ lineage **(B)** (r=-0.5386, p=0.0174, Spearman correlation). Tumor volume was positively correlated with $CD4^+$ effector memory cells **(C)** (r=0.6724, p=0.0016, Pearson correlation) and $CD8^+$ effector memory cells **(D)** (r=0.6263, p=0.0041, Spearman correlation). Tumor volume was positively associated with memory precursor effector cells of $CD4^+$ **(E)** (r=0.7451, p=0.0003, Pearson correlation) and $CD8^+$ lineages **(F)** (r=0.5737, p=0.0102, Spearman correlation).

2.3.10. Association between immune cell populations in the tumor and the spleen

Between spleen and tumor, the following immune cell distributions were found to be positively correlated: $F4/80^+$ (r=0.469, p=0.0368, Pearson correlation) (**Fig.**

2.10A), Gr-1$^+$/CD11b$^+$ MDSCs (r=0.801, p<0.0001, Spearman correlation) (**Fig. 2.10B**), CD4$^+$/CD25$^+$/FoxP3$^+$ Treg cells (r=0.702, p=0.0006, Pearson correlation) (**Fig. 2.10C**), CD4$^+$ (r=0.645, p=0.0021, Pearson correlation) (**Fig. 2.10D**), and the ratios of CD8$^+$ to Treg cells (r=0.473, p=0.0477, Pearson correlation) (**Fig. 2.10F**), CD4$^+$ to MDSC (r=0.671, p=0.0023, Pearson correlation) (**Fig. 2.10G**), CD8$^+$ to MDSC (r=0.589, p=0.0101, Spearman correlation) (**Fig. 2.10H**). CD8$^+$ was not correlated (r=0.229, p=0.3320, Spearman correlation) between spleen and tumor (**Fig. 2.10E**). The correlation analysis of all the immune cell populations in spleen and tumor included in this study is provided in **Appendix A** (**Table 4**).

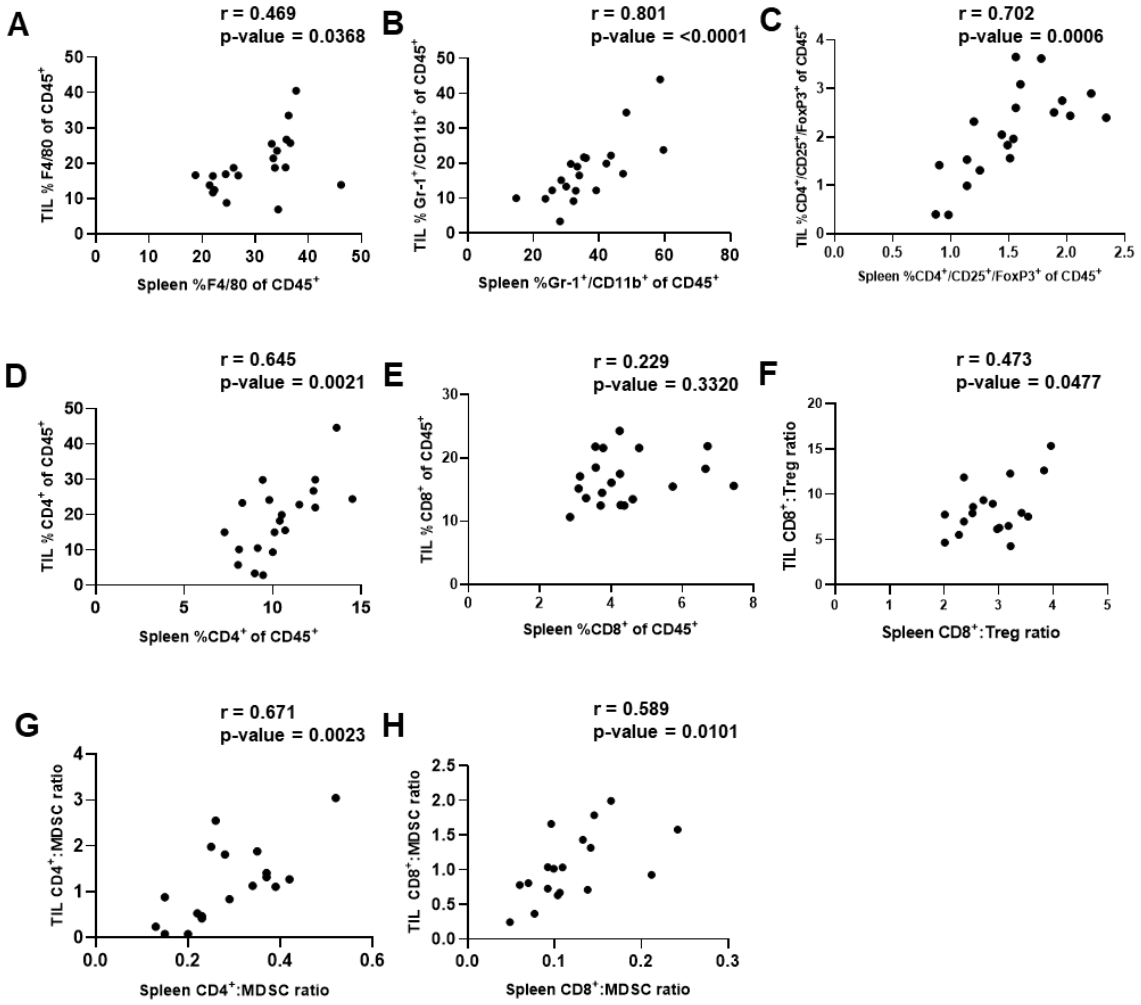

Figure 2.10. Association between immune cell populations in the tumor and the spleen. There was a significant positive association between spleen and tumor with

respect to the distribution of F4/80$^+$ **(A)** (r=0.469, p=0.0368, Pearson correlation), Gr-1$^+$/CD11b$^+$ MDSCs **(B)** (r=0.801, p<0.0001, Spearman correlation), CD4$^+$ CD25$^+$/FoxP3$^+$ T regulatory cells **(C)** (r=0.702, p=0.0006, Pearson correlation), CD4$^+$ **(D)** (r=0.645, p=0.0021, Pearson correlation), and the ratios of CD8$^+$ to T regulatory cells **(F)** (r=0.473, p=0.0477, Pearson correlation), CD4$^+$ to MDSC **(G)** (r=0.671, p=0.0023, Pearson correlation), and CD8$^+$ to MDSC **(H)** (r=0.589, p=0.0101, Spearman correlation). CD8$^+$ was not correlated (r=0.229, p=0.3320, Spearman correlation) between spleen and tumor (**E**).

2.3.11. Pilot study – Determination of experimental condition for HER2-specific IFNγ secretion by bulk culture of splenocytes

Splenocytes from mice which rejected tumors were pooled and stimulated with 10 µg/ml HER2 p63-71 peptides for 6 days of bulk culture followed by stimulation with peptides (10 µg/ml HER2 p63-71, 10 µg/ml HA p518-526, 1 µg/ml anti-CD3) or cultured with CM alone without any stimulus for 24 hours. In this assay, the mean HER2-dependent IFNγ secretion was 27.372 ng/ml and the mean HA-dependent IFNγ response was 11.950 ng/ml (**Fig. 2.11**).

In another pilot experiment, splenocytes from mice which rejected tumors were pooled and stimulated with 1x10^6 irradiated 4T1.2-HER2 cells for 6 days of bulk culture followed by stimulation with irradiated 4T1.2-HER2 cells or controls (0.4x10^6 irradiated 4T1.2 cells, 1 µg/ml anti-CD3) or cultured with CM alone without any stimulus for 24 hours. In this assay, mean IFNγ secretion from 4T1.2-HER2 cell stimulation was 13.894 ng/ml and the mean IFNγ response from 4T1.2 cell stimulation was 10.455 ng/ml (**Fig. 2.12**).

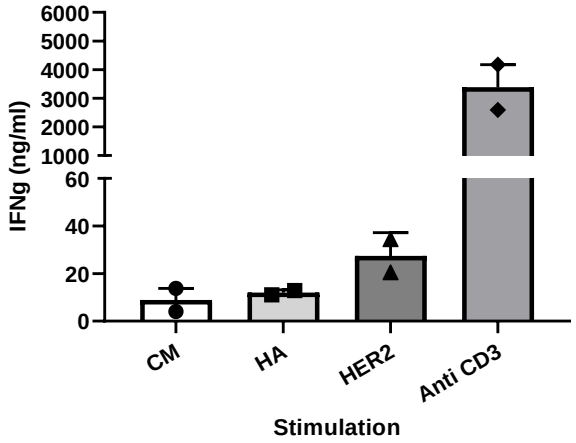

Figure 2.11. Pilot study – Determination of experimental condition for HER2-specific IFNγ response by bulk culture of splenocytes with HER2 peptide for 6 days followed by plating with stimulating peptides for 24 hours. From the mice (n=6) which did not develop tumors after inoculation of 4T1.2-HER2 cells, spleens were isolated and splenocytes of similar spleen sizes were pooled and cultured with HER2 p63-71peptide in T25 flasks for 6 days. Following the bulk culture, cells were isolated and stimulated with the 4 peptide conditions – CM (negative control), 10 µg/ml HA p518-526 (negative control), 10 µg/ml HER2 p63-71 (test), and 1 µg/ml anti-CD3 (positive control) on a 24-well plate for 24 hours. After this stimulation, supernatants were obtained and analyzed for IFNγ levels.

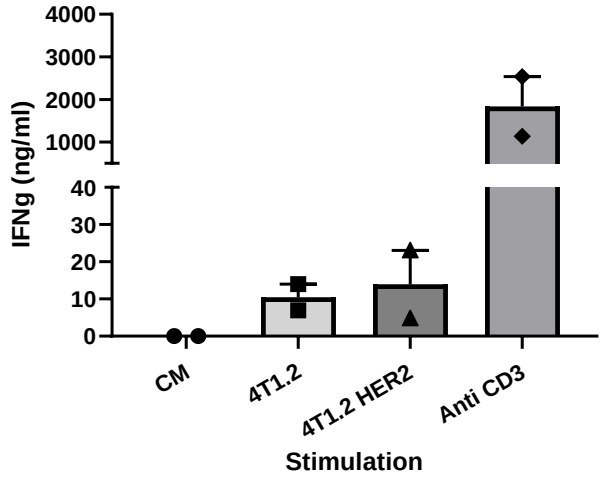

Figure 2.12. Pilot study – Determination of experimental condition for HER2-specific IFNγ response by bulk culture of splenocytes with 4T1.2-HER2 cells for 6 days followed by plating with 4T1.2-HER2 cells and appropriate controls for 24 hours. From the mice (n=6) which did not develop tumors after inoculation of 4T1.2-HER2 cells, spleens were isolated and splenocytes of similar spleen sizes were pooled and cultured with $1x10^6$ irradiated 4T1.2-HER2 cells in T25 flask for 6 days. Following the bulk culture, splenocytes were isolated and stimulated with the 4 experimental conditions – CM (negative control), $0.4x10^6$ irradiated 4T1.2 cells (negative control), $0.4x10^6$ irradiated 4T1.2-HER2 cells (test) and 1 µg/ml anti-CD3

peptide (positive control) on a 24-well plate for 24 hours. After this stimulation, supernatants were obtained and analyzed for IFNγ levels.

2.3.12. Assessment of HER2-specific IFNγ response from the splenocytes of 4T1.2-HER2 tumor-bearing mice

Spleens were isolated from tumor-bearing mice at sacrifice and the splenocytes were cultured in T25 flasks with 10 µg/ml HER2 p63-71 peptide for 6 days. Following the bulk culture, splenocytes were isolated and stimulated with peptides (10 µg/ml HER2 p63-71, 10 µg/ml HA p518-526, 1 µg/ml anti-CD3) or cultured with CM without any stimulus for 24 hours. After restimulating splenocytes following bulk culture with HER2 peptides, HER2-specific IFNγ response was not significantly different than the negative controls, HA and CM (**Fig. 2.13**). (Kruskal-Wallis Test, KW=0.3442, p=0.8419)

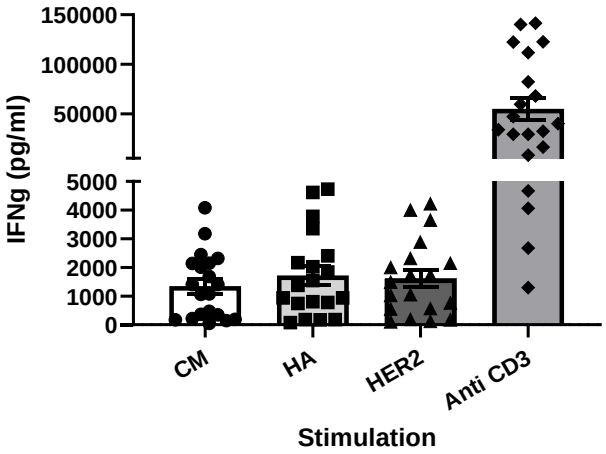

Figure 2.13. Assessment of HER2-specific IFNγ response from splenocytes in 4T1.2-HER2 tumor-bearing mice. Spleens were isolated from tumor-bearing mice at sacrifice and splenocytes were cultured in T25 flasks with 10 µg/ml HER2 p63-71 peptide for 6 days. Following the bulk culture, splenocytes were isolated and stimulated with the 4 peptide conditions – complete media (CM) only (negative control), 10 µg/ml HA p518-526 peptide (negative control), 10 µg/ml HER2 p63-71 peptide (test) and 1 µg/ml anti-CD3 (positive control) on a 24-well plate for 24 hours. After this stimulation, supernatants were obtained and analyzed for IFNγ levels. HER2-specific IFNγ response was not significantly different compared to the negative controls, HA and CM. (Kruskal-Wallis Test, KW=0.3442, p=0.8419)

2.3.13. Association between tumor volume and HER2-specific IFNγ response in the spleen

To analyze the association between tumor volume and HER2-specific IFNγ response in the spleen, the mice were stratified into two groups based on the final tumor volumes. The mice with the top 50% of tumor volumes were categorized in the high tumor volume group and the mice with the bottom 50% of tumor volumes were categorized in the low tumor volume groups. IFNγ levels from the supernatants collected after the post-bulk peptide stimulation in HER2 and HA stratified by high and low tumor volumes are shown in **Fig. 2.14**. There was no tumor volume x peptide stimulation interaction (2-way ANOVA, F(1,37)=0.1432, p=0.7072). There was no significant main effect of peptide (2-way ANOVA, F(1,37)=0.0339, p=0.8548). However, there was a trend toward the main effect of tumor volume (2-way ANOVA, F(1,37)=2.920, p=0.0959).

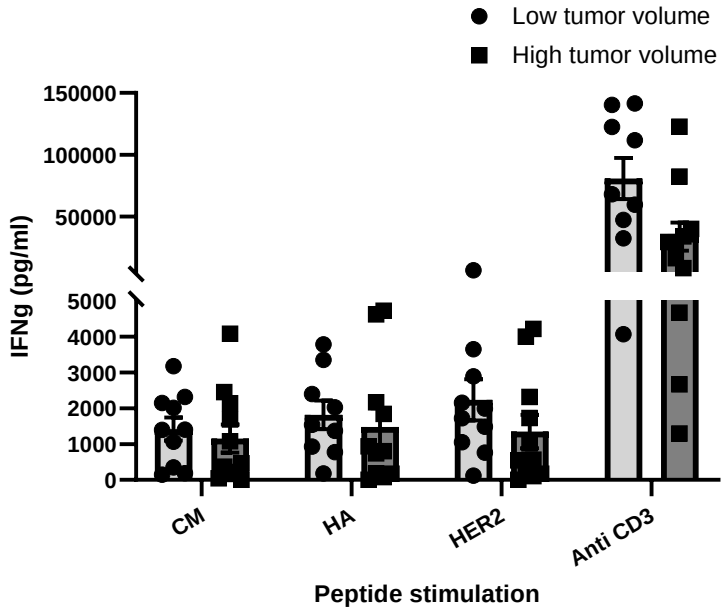

Figure 2.14. Association between tumor volumes and HER2-specific IFNγ responses in the spleen. To analyze the association between tumor volume and HER2-specific IFNγ response in the spleen, the mice were stratified into two groups based on final tumor volumes as high tumor volumes or low tumor volumes. IFNγ

levels from the supernatants collected after the post-bulk stimulation with HER2 and HA were compared between the two tumor volume groups by 2-way ANOVA. There was no tumor volume x peptide stimulation interaction effect (2-way ANOVA, F(1, 37) = 0.1432, p=0.7072). There was no significant main effect of peptide (2-way ANOVA, F(1, 37) = 0.033, p=0.8548). However, there was a marginal main effect of tumor volume (2-way ANOVA, F(1, 37) = 2.920, p=0.0959).

2.3.14. Assessment of HER2-specific IFNγ response from the TILs of 4T1.2-HER2 tumor bearing mice

Tumors were isolated from mice at sacrifice and the cells from tumors were cultured with peptides (10 µg/ml HER2 p63-71, 10 µg/ml HA p518-526, 1 µg/ml anti-CD3) or cultured with CM without any stimulus in a 24-well plate for 48 hours. Supernatants were obtained from these cultures after 48 hours and analyzed for IFNγ levels. From the 48-hour culture of tumor cells with stimulating peptides, IFNγ response was significantly increased in the HER2 stimulation group compared to the negative controls, CM and HA (**Fig. 2.15**). (Kruskal-Wallis test, KW=10.05, p=0.0066).

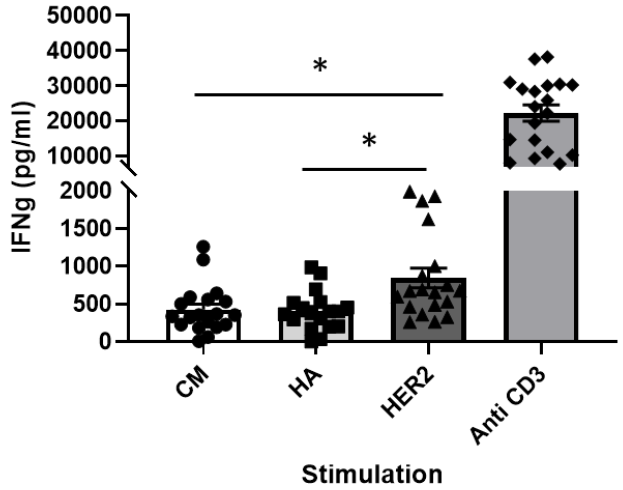

Figure 2.15. Assessment of HER2-specific IFNγ response from the TILs of 4T1.2-HER2 tumor-bearing mice. Tumors were isolated from mice at sacrifice and cells from the tumor were plated with 4 peptide stimulation conditions – complete media (CM) only (negative control), 10 µg/ml HA p518-526 (negative control), 10 µg/ml HER2 p63-71 and 1 µg/ml anti-CD3 (positive control) on a 24-well plate for 48 hours. Supernatants were obtained from these cultures after 48 hours and analyzed for IFNγ

levels. HER2-specific IFNγ response was significantly increased compared to the negative controls, CM and HA. (Kruskal-Wallis test, KW=10.05, p=0.0066)

2.3.15. Association between tumor volume and HER2-specific IFNγ responses in the tumor

To analyze the association between tumor volumes and HER2-specific immune response in the tumors, the mice were stratified into two groups based on final tumor volumes. The mice with the top 50% of tumor volumes were categorized in the high tumor volume group, and the mice with the bottom 50% of tumor volumes were categorized in the low tumor volume groups. Differences in IFNγ levels from the supernatants obtained in the 48-hour peptide stimulation from HER2 and HA were compared between the high and low tumor volume groups using 2-way ANOVA (**Fig. 2.16**). There was a significant main effect of tumor volume (2-way ANOVA, $F(1,35)=4.703$, $p=0.0370$). There was a significant main effect of peptide (2-way ANOVA, $F(1, 35)=4.412$, $p=0.0430$).There was a marginal tumor volume x peptide stimulation interaction (2-way ANOVA, $F(1,35)=2.915$, $p=0.0966$). HER2-specific IFN-γ response was higher compared to HA-specific IFN-g response in mice with low tumor volume but not high tumor volume (Dunnett's multiple comparisons test, $p=0.0265$).

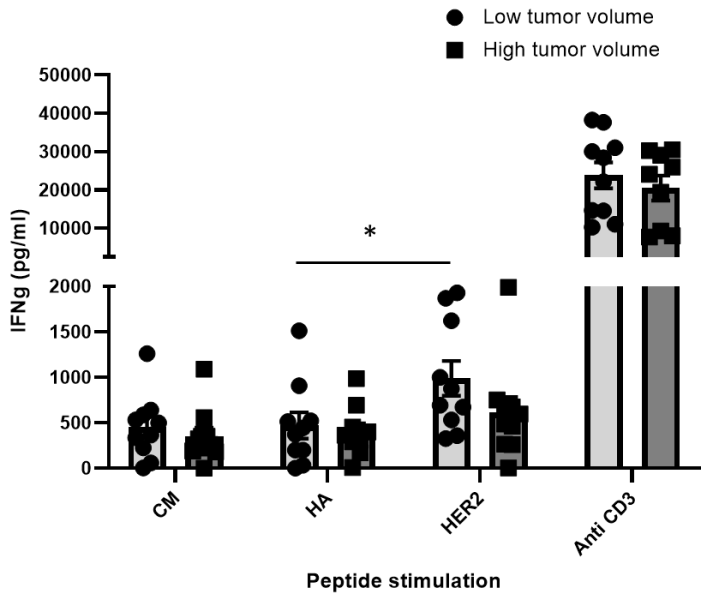

Figure 2.16. Association between tumor volumes and HER2-specific IFNγ responses in the tumor. To analyze the association between HER2-specific IFNγ response in the tumor and tumor volumes, the tumors were stratified into two groups based on final volumes as low and high tumor volume groups. IFNγ levels from the supernatants of immune cells from the tumor cultured for 48-hours with HER2 and HA were compared between the two tumor volume groups by 2-way ANOVA. There was a significant main effect of tumor volume (2-way ANOVA, F(1,35)=4.703, p=0.0370). There was a significant main effect of peptide (2-way ANOVA, F(1, 35)=4.412, p=0.0430).There was a marginal tumor volume x peptide stimulation interaction (2-way ANOVA, F(1,35)=2.915, p=0.0966). HER2-specific IFNγ response was higher compared to HA-specific IFNγ response in mice with low tumor volume but not in mice with high tumor volume (Dunnett's multiple comparisons test, p=0.0265).

2.3.16. Assessment of lung metastasis in the 4T1.2-HER2 tumor model using the gene expression of gp70

To assess the presence of lung metastasis, lungs were isolated from the mice (n=35) at sacrifice. The gene expression of gp70 was analyzed using RT-PCR. From the Cycle threshold (Ct) values of gp70 (**Fig. 2.17**), all the tumor bearing mice (each mouse has been denoted with the prefix, “M”) had metastasis to the lungs. In the control mice (denoted by ctrl), the gene expression of gp70 was absent. Of the 35 tumor-bearing mice analyzed, 22 had a strong positive gene expression of gp70 and 13 had a positive gene expression (**Table 2.2**). (Reference ranges: Cts < 29 - strong

positive reactions; Cts in the range of 30-37 - positive reactions; Cts in the range of 38-40 - weak reactions)

Table 2.2. Gene expression levels of gp70 in mice based on Ct values. (Reference ranges for Ct values: Cts < 29 - strong positive reactions; Cts in the range of 30-37 - positive reactions; Cts in the range of 38-40 - weak reactions)

Gene expression level of gp70	No. of mice (n total = 35)
Strongly positive	22
Positive	13
Weakly positive	0

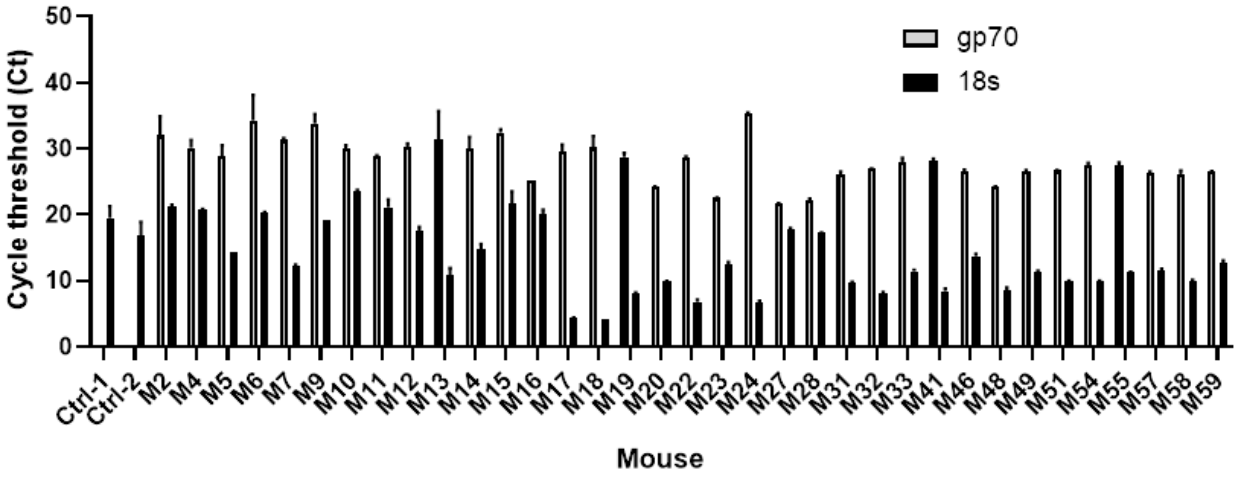

Figure 2.17. Assessment of lung metastasis in the 4T1.2-HER2 tumor model using the gene expression of gp70. Lungs were isolated from mice (n=35) at sacrifice. Gene expression of gp70 was analyzed using RT-PCR in 35 tumor bearing mice (denoted with M) and two control mice (denoted with Ctrl-1 and 2).

2.3.17. Association between lung metastasis and tumor volume in the 4T1.2-HER2 tumor model

To assess the relationship of lung metastasis with tumor volume, the mice (n=35) were stratified into two groups based on their tumor volumes at sacrifice and their ΔCt values of gp70 (Ct_{gp70} – Ct_{18s}) were compared (**Fig. 2.18**). There was no

significant difference in lung metastasis between the mice with low or high tumor volumes (Mann-Whitney test, p=0.9870).

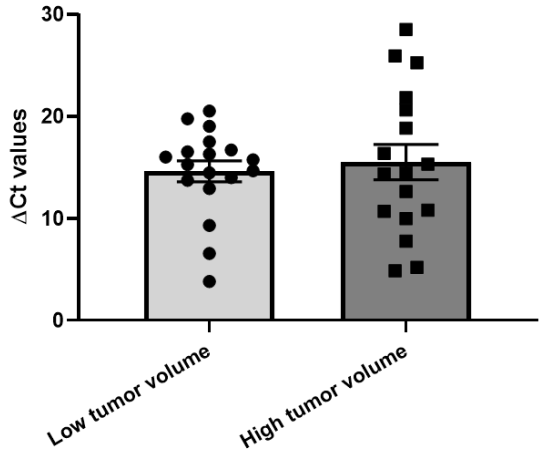

Figure 2.18. Association between lung metastasis and tumor volume in the 4T1.2-HER2 tumor model. There was no significant difference in the ΔCt values of gp70 (Ct_{gp70}-Ct_{18s}) between mice with smaller and larger tumor volumes at sacrifice. (n=35, Mann-Whitney test, p=0.9870)

2.3.18. Immune cells associated with HER2-specific IFNγ secretion in the spleen and tumor

The focus of this study was to understand the primary tumor growth, immune responses, and metastasis in the 4T1.2-HER2 tumor model. Additionally, an exploratory analysis was carried out to identify the immune cells that influence HER2-specific immune response in the spleen and tumor. A correlation analysis was performed between the immune cells present in the spleen and tumor and the HER2 antigen specific IFNγ response. The results are shown in **Appendix B**.

In the spleen, HER2-specific IFNγ secretion was negatively correlated with mMDSC cells (**Fig. 1A**) (r=-0.681, p=0.002, Pearson correlation) and positively correlated with $CD4^+$ lymphocytes (**Fig. 1B**) (r=0.437, p=0.054, Pearson correlation), and NK cells (**Fig. 1C**) (r=0.495, p=0.026, Spearman correlation).

In the tumor, HER2-specific IFNγ secretion was negatively correlated with MDSCs (**Fig. 2B**) (r=-0.514, p=0.020, Spearman correlation) and positively correlated with total $CD45^+$ cells (**Fig. 2A**) (r=0.493, p=0.027, Spearman correlation), $CD4^+$ (**Fig. 2C**) (r=0.452, p=0.045, Spearman correlation), $CD4^+$:$CD8^+$ ratio (**Fig. 2D**) (r=0.510, p=0.022, Spearman correlation), and $CD4^+$:Treg cell ratio (**Fig. 2E**)(r=0.525, p=0.017, Spearman correlation). The correlation analysis of all the immune cell populations included in this study are provided in **Appendix B** (**Table 5**, **Table 6**, and **Table 7**).

2.4. DISCUSSION

Preclinical mouse models of breast cancer that can replicate the human disease phenotype can serve as valuable tools for breast cancer research. The 4T1.2 tumor model, a commonly used transplantable breast cancer, has the disadvantage of being poorly immunogenic, which makes immune studies in this model difficult. To overcome this drawback, a surrogate antigen, HER2, was transduced into the 4T1.2 cell line. A previous study demonstrated the involvement of HER2-specific CTL in mediating tumor regression in the subcutaneously implanted 4T1.2-HER2 cells (113). Thus, we undertook experiments in our lab to characterize this tumor model using an orthotopic injection of tumor cells into the mammary gland with the aim of studying immune outcomes and metastatic properties.

We previously observed that 4T1.2-HER2 exhibited a three-phased growth pattern with a short period of initial tumor growth followed by spontaneous tumor regression and a third phase of heterogeneous tumor growth with some mice showing increased tumor growth and some mice rejecting the tumors. We previously characterized the immune responses in the early phase of tumor growth. From these experiments, we discovered the presence of HER2-specific IFNγ secretion in tumor-

infiltrating lymphocytes and observed that antitumor immune cell infiltration in spleen and tumor was associated with tumor regression (115).

The goal of the current study was to determine if HER2-specific immune responses are involved in mediating tumor regression in the later phase. Based on our previous studies (115), we hypothesized that increased primary tumor growth would be positively associated with the suppression of antitumor immune responses and greater metastatic burden.

When the tumor cells were inoculated in mice, tumor growth pattern was seen in three phases. While this three-phased tumor growth pattern was quite similar to the previous studies conducted in our lab, there were significant differences in tumor growth compared to the previous study. In the earlier studies, a sharp regression in tumor growth was observed between day 10 – day 20. In the present study, there was either a mild tumor growth regression or stagnation in the growth. In the previous studies, during the third phase, some mice rejected tumors, while others developed large or intermediate size tumors. However, in the present study, none of the mice rejected tumors in the third phase of tumor growth, but heterogeneous tumor growth patterns were observed in the current study.

Comparative analysis of the data collected from the present study with the previous studies suggests that aging could cause an increase in tumor growth to some extent in this tumor model. Due to aging, immune system dysfunction can occur, and this can have adverse effects on the tumor growth (118). Some effects of aging on the immune system include decreased naïve T cell population, decreased TCR repertoire diversity, and a decreased antigen presenting cell capacity by dendritic cells (119, 120). Although increased average tumor growth and an increased recurrence in the

later phase could be attributed to aging, it does not explain all of the observed rise in tumor growth seen in this study.

The increase in tumor volume in the current study may also be explained by differences in housing or lab environment or the development of new tumor cell variants within the primary tumor. Previous studies indicate that environmental factors such as housing conditions or usage of different labs could cause differences in tumor outcomes (121). In this study, the mice were group housed, whereas in the previous study, the mice were singly housed. Group housing may induce social hierarchy, affect access to food, water, nesting, or may make the mice more prone to trauma at the tumor site from grooming or biting. All of these factors might affect tumor growth directly by altering TME or indirectly through immune alteration (122-126). Mice in the current study were housed in the Chandlee Laboratory Animal Facility and mice from the previous study were housed in the South Frear Animal Facility. Previous studies show that tumor growth differences occur when mice are housed in different animal facilities, despite otherwise controlled conditions (i.e., food, temperature, tumor cell lines, etc.) (121, 127).

Tumor cells have the potential to alter their cell surface molecule expression, and it is one of their immune evasion strategies (59, 128). Other studies have found that tumor cells can evade immune recognition by the loss of MHC I molecules or loss of tumor antigen (128-130). A colon carcinoma cell line that expresses HER2, CT26/HER2 exhibited variants while growing *in vivo* in mice and resisted HER2-based immune responses (130). In our study, due to selective pressure *in vivo*, there is a possibility that the tumor cells may have downregulated expression of HER2, which potentially enabled greater resistance to immune recognition and facilitated increased

tumor growth. Further studies are necessary to understand the confounding factors associated with increased tumor growth in this study.

In both spleen and tumor, to understand the association between immune cell distribution and tumor volume, correlation analyses were performed. The percentage of dendritic cells in the spleen had a significant negative association with tumor volume. Dendritic cells in the tumor were not associated with tumor volume. Potential DC dysfunction, decreased DC infiltration or immunosuppression in the TME might explain the lack of association of DC in tumor with tumor volume in our study. Tumor-infiltrating dendritic cells have low co-stimulatory molecule expression and antigen presentation capacity (131). In a study conducted with 60 breast cancer patients, plasmacytoid dendritic cells (pDC) from tumors secreted less IFNα compared to pDC collected from patients' blood (132).

Among the effector cells, the percentage of $CD4^+$ and NK cells in the tumors had a negative association with tumor volume. $CD4^+$ T cells mediate antitumor immune responses by serving as T helper cells and they help in activation and expansion of $CD8^+$ T cells and generation of memory CD8 cells. (70). Although $CD4^+$ T cell function has not been evaluated specifically in TNBC, T_H1 and T_{FH} subtypes have been associated with better survival outcomes in breast cancer (85, 90). NK cells are cytotoxic against tumor cells (52, 59). Increased expression of NK cell activating genes in the tumor has been associated with decreased recurrence in breast cancer patients (85). Despite the infiltration of $CD8^+$ T cells in the tumor and a previous study suggesting the involvement of these cells in HER2-specific response (113), it was surprising to observe no association of $CD8^+$ T cells in the spleen or tumor with tumor volume. $CD4^+$:$CD8^+$ ratio in the tumors was negatively associated with tumor volume,

and this ratio might suggest a greater association of CD4 rather than CD8 with the tumor volume.

Tregs have been conventionally associated with immunosuppressive functions (52). However, data in TNBC patients indicate that a greater level of Tregs in tumors is associated with a better prognosis (96). Interestingly, our study reflected similar findings. The percentage of Tregs in the spleen and tumors had a significant negative association with tumor volume. Further, the ratio of $CD4^+$:Treg in tumors had a positive association with tumor volume, and this ratio could have been driven positively as a result of a greater negative association of Treg with tumor volume.

MDSCs are associated with tumor burden in many murine breast cancer models as well as in breast cancer patients (133, 134). In the peripheral blood of breast cancer patients, MDSCs increase in a step-wise manner based on the breast cancer stage of the patient from 1.96% in stage I/II to 2.46% and 3.77% in stage III and IV, respectively. Furthermore, in stage IV patients with metastasis in three or more organs, the MDSC levels increase to 4.37% (102). Consistent with clinical findings, we observed a significant positive correlation of MDSCs in both spleen and tumors with tumor volume. Among the MDSC subtypes in the spleen, gMDSCs were greater in numbers compared to mMDSCs, but mMDSCs had a significant positive correlation with the tumor volume. In a preclinical study examining MDSC subtypes in ten mouse tumor models, spleens had a greater increase of gMDSCs compared to mMDSCs (135). On a per cell basis, mMDSCs have a greater suppressive potential compared to gMDSCs (136). $CD4^+$:MDSC and $CD8^+$:MDSC cell ratios were strongly negatively correlated in the tumors. These increased negative cell ratio associations are likely driven by a greater positive association of MDSC than an increased negative T cell association.

Central memory cells in the tumor were negatively correlated with tumor volume. Previous findings show that T_{CM} produce higher levels of cytokines, exert stronger cytotoxic activity and have greater efficacy on a per cell basis compared to effector T cells (137, 138). Further, central memory cells have a longer life span than effector cells, and Tregs have less ability to inhibit them (139). In early-stage colorectal cancer, central memory T cells are associated with increased survival and decreased recurrence (140). Clinical studies in breast cancer have been undertaken with resident memory T cells (T_{RM}) which express CD103 albeit with a similar cytokine profile of T_{CM}. T_{RM}, which localize in tumor parenchyma, have been associated with greater risk-free survival in breast cancer (141). It is not clearly understood why effector memory cells and memory precursor effector cells were positively associated with tumor volumes. Further, there was a significant negative correlation between $CD4^+$ and $CD8^+$ T_{EM} and HER2-specific IFNγ secretion (**Appendix B**, **Table 7**). Further studies are needed to explain these associations which are contradictory to the reported immune functions of these cell types (138).

For optimizing the culture conditions to determine HER2-specific IFNγ secretion in the spleen, pilot studies were done. Bulk culture with HER2 peptide p63-71 rather than irradiated 4T1.2-HER2 tumor cells gave optimal HER2-specific IFNγ secretion responses. In the main study, ex vivo stimulation of immune cells from the tumor with $H\text{-}2K^d$-restricted HER2 peptide for 48h induced HER2-specific IFNγ secretion. Further, analysis of IFNγ secretion with tumor volume revealed the presence of HER2-specific IFNγ secretion only in smaller size tumors. The finding indicates that the observed anti-HER2 immune response from tumor-infiltrating immune cells from mice with small tumors may be the cause or consequence of smaller tumor sizes. This finding indicates that significant antigen-specific response against HER2 occurs in the late

stages of tumor growth in the 4T1.2-HER2 tumor model. Thus, the transduction of the HER2 gene into the 4T1.2 tumor cells alters the cell's immunogenicity and stimulates HER2-specific immune responses. Observation of these findings only in the tumors and not in the spleens might indicate the presence of divergent immune responses in the tumor and spleen. Further, it is suggestive of the presence of greater HER2-specific immune responses in the tumors than in the spleen.

Among breast cancer subtypes, TNBC is the most immunogenic due to the presence of increased mutational load, which increases their antigenic signatures (87, 142). Findings from our study indicate that the 4T1.2-HER2 tumor model is more immunogenic than the 4T1.2 tumor model and could serve as a better model for TNBC.

gp70 is a viral envelope glycoprotein that is transcriptionally silent in normal murine tissues. The expression of gp70 is reactivated in several murine tumor cell lines (143). Since gp70 is expressed in the tumor cells, the gene expression of gp70 was used as a marker for metastasis in the lung. We observed lung metastasis in all the mice in this experiment. Some mice showed strong positive expression and some showed moderate positive expression. This confirms that despite the insertion of HER2 into the genome, lung metastasis still occurs in this tumor model. Further, we did not observe any linear relationship between tumor volume and lung metastasis using gp70 gene expression as a biomarker for lung metastasis. This could potentially be due to a high level of metastatic burden in all the mice at the late stage of tumor growth, which masked the relation between tumor volume and metastasis, or due to increased assay sensitivity or a combination of the two.

In summary, from the experiments conducted to characterize the late stages of tumor growth in the 4T1.2-HER2 tumor model, we found that the addition of HER2 to the 4T1.2 tumor cell line significantly changed the original growth trajectory of the

parental cell line by altering the tumor cell's immunogenicity. The growth was observed in three phases, with an increase in tumor growth in the first and third phases, and regression in the second phase. In this study, we characterized the third phase, in which we observed an association of antitumor immune cells such as APCs and effector cells with a decrease in tumor growth and a significant association of immunosuppressive MDSCs with an increase in tumor growth. Further, we observed a significant antigen-specific IFNγ response in the tumor against HER2 peptide, and this response was seen only in smaller tumor volumes and not in larger tumor volumes. All the mice exhibited lung metastasis at the time of sacrifice. We did not observe any linear relation of tumor growth with lung metastasis at the late stage using gp70 gene expression to detect metastasis.

CHAPTER 3: CONCLUSION AND FUTURE DIRECTIONS

From the earlier studies undertaken to characterize the 4T1.2-HER2 tumor model in our laboratory, we observed that the addition of HER2 to the parental 4T1.2 model greatly increased its immunogenicity by acting as a tumor antigen. The *in vivo* tumor growth pattern of the 4T1.2-HER2 tumor model had three phases of tumor growth. In the early stages of tumor growth, antitumor immune responses were associated with tumor regression, and immunosuppression was associated with tumor growth. The objective of the current study was to characterize tumor growth, immune outcomes, and metastatic burden in the late stage of tumor growth. Based on the findings from earlier studies (43, 115), we hypothesized that increased primary tumor growth would be positively associated with the suppression of antitumor immune responses and greater metastatic burden.

For Aim 1, we wanted to determine if tumor volume is associated with immune cell infiltration. In this aim, we hypothesized that larger tumor volume at sacrifice would be negatively associated with antitumor immune cell infiltration and positively associated with immunosuppressive cell infiltration, and smaller tumor volume at sacrifice will be positively associated with antitumor immune cell infiltration and negatively associated with immunosuppressive cell infiltration.

We found that cells involved in antitumor responses such as dendritic cells in the spleen and $CD4^+$ T cells, NK cells, and central memory cells in the tumor were negatively associated with tumor volume. We also found that MDSCs in the spleen and tumor and mMDSCs in the spleen were positively associated with tumor volumes. These findings are consistent with our hypothesis. However, it was surprising that cytotoxic $CD8^+$ T cells, which are important in the antitumor response, were not correlated with tumor volumes. Further, in the case of Tregs, we observed a negative

correlation with tumor volume in both spleen and tumor. There is evidence of a favorable prognosis with increased Tregs from clinical breast cancer data (85), but a traditional immunosuppressive role is attributed to Tregs (52). With regard to the effector memory and memory precursor effector cells, their role in cancer is not well characterized. One of the limitations of the current study is that we did not functionally evaluate the immune cell subtypes. Thus, we cannot conclusively state whether Treg, effector memory and memory precursor effector cell data support or refute our hypothesis.

For Aim 2, we wanted to determine if tumor volume is associated with HER2 antigen-specific IFNγ secretion. In this aim, we hypothesized that smaller tumor volume at sacrifice would be associated with increased HER2-specific IFNγ secretion, and larger tumor volume at sacrifice will be associated with decreased HER2-specific IFNγ secretion. In the tumors, we observed HER2-specific responses only in smaller tumor volumes and this response was not seen in larger tumor volumes. The data from tumors supports this hypothesis, albeit with a marginal significance. However, in the spleen, we found only a trend towards greater IFNγ response in smaller tumor volumes. The data from spleen does not conclusively support this hypothesis.

For Aim 3, we wanted to determine if tumor volume is associated with metastatic burden in the lungs. We hypothesized that larger tumor volume at sacrifice would be associated with an increased metastatic burden, and smaller tumor volume at sacrifice will be associated with a decreased metastatic burden. Using gp70 gene expression as a biomarker for lung metastasis, we did not observe any linear relationship between tumor volume and lung metastasis.

In the current study, we comprehensively characterized the immune cell outcomes, HER2-specific immune responses, and lung metastatic burden in the late stages of tumor growth in the 4T1.2-HER2 tumor model. After the completion of the current study, some questions still remain regarding the tumor growth outcomes, the role of immune cells and lung metastasis.

Factors affecting tumor growth need to be studied further to ensure the reproducibility of results. Questions about the involvement of housing conditions, lab environment, and the loss of HER2 antigen in promoting tumor growth have to be followed up with future studies. Designing future experiments with similar housing and laboratory conditions might ensure better reproducibility of the tumor data.

In this study, we assessed the correlation of immune cells with tumor outcomes. Correlations do not necessarily imply a causative role. Further, the findings about Tregs, effector memory cells, and memory precursor effector cells were contradictory to their reported functions. To understand the associative data in a better way, functional studies need to be undertaken to characterize the role of Tregs, effector memory cells, and memory precursor effector cells in the context of breast cancer.

In this study, we did not observe a linear relationship between lung metastasis and tumor growth using gp70 gene expression. There is greater metastatic burden at late stages of tumor growth which might confound this relation. Repetition of this experiment at an early stage could provide a better assessment of the relationship between primary tumor growth and lung metastasis.

Data from the current study and other studies undertaken by our laboratory to characterize the 4T1.2-HER2 tumor model have furthered our understanding of this tumor model, particularly in the context of immune responses. This model could be an ideal experimental system to study antigen-specific immune responses in

immunotherapeutic as well as for intervention-based experiments in breast cancer. Our laboratory is interested in investigating the immune mechanisms underlying the effects of exercise and energy restriction interventions on breast cancer using pre-clinical mouse models. This tumor model would help us explore whether exercise and energy restrictions can alter antigen-specific immune responses in breast cancer.

APPENDIX A. CORRELATION OF IMMUNE CELLS WITH TUMOR VOLUMES

Table 1. Association between immune cell populations in the spleen and final tumor volume.

Immune cell type	Pearson's or Spearman's r	p-value
%$CD45^+$ of total	0.389	0.100
%$F4/80^+$ of $CD45^+$	-0.343	0.128
%$F4/80^+$ $CD11b^+$ of $CD45^+$	-0.081	0.726
%$I\text{-}Ad^+$ $CD11b^+$ of $CD45^+$	-0.492	0.024
%$I\text{-}Ad^+$ $CD11c^+$ of $CD45^+$	-0.653	0.001
%$Gr\text{-}1^+$ $CD11b^+$ of $CD45^+$	0.598	0.004
%gMDSC of $CD45^+$	0.184	0.425
%mMDSC of $CD45^+$	0.597	0.006
%$CD4^+$ of $CD45^+$	-0.246	0.282
%$CD8^+$ of $CD45^+$	-0.301	0.184
%NK cells of $CD45^+$	-0.294	0.197
%$CD4^+$ $CD25^+$ $FoxP3^+$ of $CD45^+$	-0.458	0.037
CD4:CD8	0.383	0.087
CD4:MDSC	-0.432	0.057
CD8:MDSC	-0.408	0.075
gMDSC:mMDSC	-0.430	0.052
CD4:Treg	0.555	0.009
CD8:Treg	0.235	0.305

Table 2. Association between immune cell populations in the tumor and final tumor volume.

Immune cell type	Pearson's or Spearman's r	p-value
%$CD45^+$ of total	-0.060	0.801
%$F4/80^+$ of $CD45^+$	-0.276	0.238
%$F4/80^+$ $CD11b^+$ of $CD45^+$	0.335	0.148
%$I\text{-}Ad^+$ $CD11b^+$ of $CD45^+$	0.023	0.925
%$I\text{-}Ad^+$ $CD11c^+$ of $CD45^+$	-0.153	0.519
%$Gr\text{-}1^+$ $CD11b^+$ of $CD45^+$	0.556	0.011
%gMDSC of $CD45^+$	0.456	0.078
%mMDSC of $CD45^+$	-0.192	0.460
%$CD4^+$ of $CD45^+$	-0.565	0.0094
%$CD8^+$ of $CD45^+$	-0.363	0.1155
%NK cells of $CD45^+$	-0.536	0.018
%$CD4^+$ $CD25^+$ $FoxP3^+$ of $CD45^+$	-0.661	0.0015
CD4:CD8	-0.529	0.017
CD4:MDSC	-0.623	0.004
CD8:MDSC	-0.612	0.005
gMDSC:mMDSC	0.335	0.242
CD4:Treg	-0.165	0.486
CD8:Treg	0.435	0.071

Table 3. Association between effector and memory cells in the tumor and final tumor volume.

Immune cell type		Pearson's or Spearman's r	p-value
% of $CD4^+$ T cells	$\%CD69^+$	0.197	0.418
	$\%PD\text{-}1^+$	0.312	0.194
	$\%CD44^-CD62L^+$(naïve)	-0.402	0.088
	$\%CD44^-CD62L^-$(EC)	0.066	0.789
	$\%CD44^+CD62L^+$ (T_{CM})	-0.619	0.005
	$\%CD44^+$ $CD62L^-$(T_{EM})	0.672	0.002
	$\%KLRG1^-$ $CD127^-$(EEC)	-0.001	0.996
	$\%KLRG1^-CD127^+$(MPEC)	0.745	0.000
	$\%KLRG1^+CD127^-$(SLEC)	0.204	0.403
	$\%KLRG1^+CD127^+$(DPEC)	0.294	0.251
% of $CD8^+$ T cells	$\%CD69^+$	0.222	0.361
	$\%PD\text{-}1^+$	0.234	0.335
	$\%CD44^-CD62L^+$(naïve)	-0.431	0.074
	$\%CD44^-CD62L^-$(EC)	-0.145	0.554
	$\%CD44^+CD62L^+$ (T_{CM})	-0.539	0.017
	$\%CD44^+$ $CD62L^-$(T_{EM})	0.626	0.004
	$\%KLRG1^-$ $CD127^-$(EEC)	0.229	0.346
	$\%KLRG1^-CD127^+$(MPEC)	0.574	0.010
	$\%KLRG1^+CD127^-$(SLEC)	0.317	0.186
	$\%KLRG1^+CD127^+$(DPEC)	-0.140	0.593

Table 4. Association between immune cell populations in the tumor and the spleen.

Immune cell type	Pearson's or Spearman's r	p-value
%$CD45^+$ of total	-0.196	0.435
%$F4/80^+$ of $CD45^+$	0.469	0.037
%$F4/80^+$ $CD11b^+$ of $CD45^+$	0.237	0.315
%$I\text{-}Ad^+$ $CD11b^+$ of $CD45^+$	0.159	0.502
%$I\text{-}Ad^+$ $CD11c^+$ of $CD45^+$	0.382	0.097
%$Gr\text{-}1^+$ $CD11b^+$ of $CD45^+$	0.801	<0.0001
%gMDSC of $CD45^+$	-0.047	0.863
%mMDSC of $CD45^+$	0.114	0.661
%$CD4^+$ of $CD45^+$	0.645	0.002
%$CD8^+$ of $CD45^+$	0.229	0.332
%NK cells of $CD45^+$	0.397	0.093
%$CD4^+$ $CD25^+$ $FoxP3^+$ of $CD45^+$	0.702	0.001
CD4:CD8	-0.180	0.449
CD4:MDSC	0.671	0.002
CD8:MDSC	0.589	0.010
gMDSC:mMDSC	-0.139	0.636
CD4:Treg	-0.157	0.509
CD8:Treg	0.473	0.048

APPENDIX B. CORRELATION OF IMMUNE CELLS WITH HER2-SPECIFIC IFNγ RESPONSE

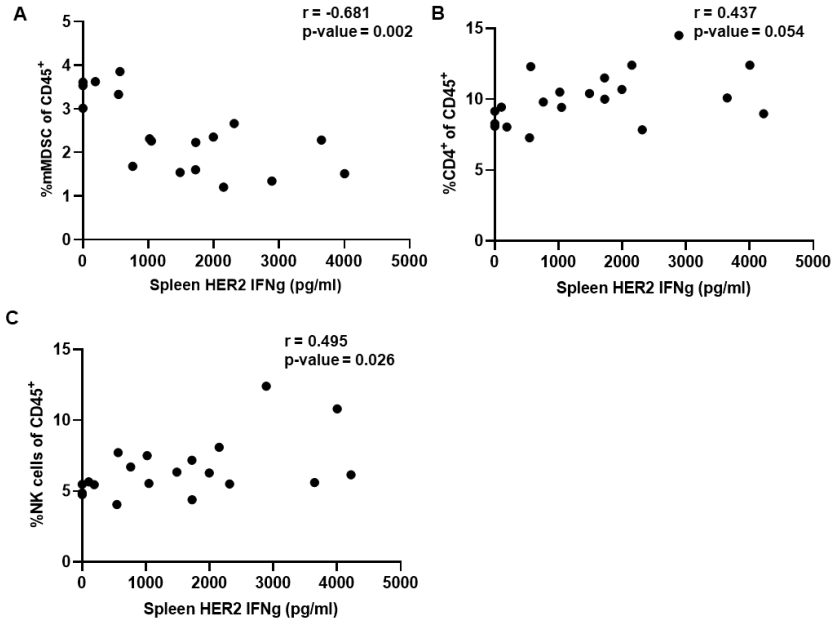

Figure 1. Association of immune cells in the spleen with HER2-specific IFNγ response. In the spleen, HER2-specific IFNγ secretion was negatively correlated with CD11b^{+} Ly6C^{hi} Ly6G^{-} mMDSC cells **(A)** (r=-0.681, p=0.002, Pearson correlation) and positively correlated with CD4^{+} lymphocytes **(B)** (r=0.437, p=0.054, Pearson correlation), and NK cells **(C)** (r=0.495, p=0.026, Spearman correlation)

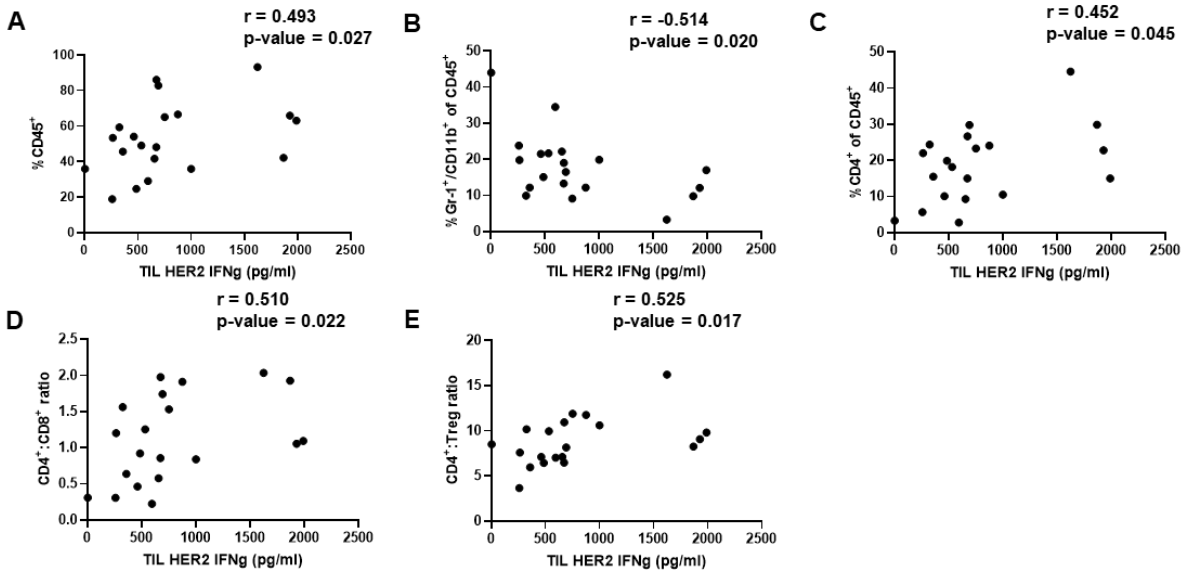

Figure 2. Association of immune cells in the tumor with HER2-specific IFNγ response. In the tumor, HER2-specific IFNγ secretion was negatively correlated with Gr-1^{+} CD11b^{+} MDSCs **(B)** (r=-0.514, p=0.020, Spearman correlation) and positively correlated with CD45^{+} **(A)** (r=0.493, p=0.027, Spearman correlation), CD4^{+} **(C)**

(r=0.452, p=0.045, Spearman correlation), $CD4^+$:$CD8^+$ ratio **(D)** (r=0.510, p=0.022, Spearman correlation), $CD4^+$:T regulatory cell ratio **(E)** (r=0.525, p=0.017, Spearman correlation).

Table 5. Association of immune cells in the spleen with HER2-specific IFNγ response.

Immune cell type	Pearson's or Spearman's r	p-value
%$CD45^+$ of total	0.103	0.685
%$F4/80^+$ of $CD45^+$	-0.041	0.227
%$F4/80^+$ $CD11b^+$ of $CD45^+$	-0.220	0.864
%$I\text{-}Ad^+$ $CD11b^+$ of $CD45^+$	0.190	0.352
%$I\text{-}Ad^+$ $CD11c^+$ of $CD45^+$	0.172	0.421
%$Gr\text{-}1^+$ $CD11b^+$ of $CD45^+$	-0.235	0.468
%gMDSC of $CD45^+$	-0.080	0.737
%mMDSC of $CD45^+$	-0.681	0.002
%$CD4^+$ of $CD45^+$	0.437	0.054
%$CD8^+$ of $CD45^+$	0.279	0.234
%NK cells of $CD45^+$	0.495	0.026
%$CD4^+$ $CD25^+$ $FoxP3^+$ of $CD45^+$	0.245	0.297
CD4:CD8	-0.036	0.880
CD4:MDSC	0.319	0.183
CD8:MDSC	0.399	0.091
gMDSC:mMDSC	0.183	0.441
CD4:Treg	0.067	0.779
CD8:Treg	0.068	0.776

Table 6. Association of immune cells in the tumor with HER2-specific IFNγ response.

Immune cell type	Pearson's or Spearman's r	p-value
%$CD45^+$ of total	0.493	0.027
%$F4/80^+$ of $CD45^+$	0.022	0.927
%$F4/80^+$ $CD11b^+$ of $CD45^+$	-0.415	0.069
%$I\text{-}Ad^+$ $CD11b^+$ of $CD45^+$	-0.314	0.178
%$I\text{-}Ad^+$ $CD11c^+$ of $CD45^+$	-0.107	0.654
%$Gr\text{-}1^+$ $CD11b^+$ of $CD45^+$	-0.514	0.020
%gMDSC of $CD45^+$	0.174	0.520
%mMDSC of $CD45^+$	-0.368	0.146
%$CD4^+$ of $CD45^+$	0.452	0.045
%$CD8^+$ of $CD45^+$	-0.136	0.567
%NK cells of $CD45^+$	-0.032	0.898
%$CD4^+$ $CD25^+$ $FoxP3^+$ of $CD45^+$	0.185	0.435
CD4:CD8	0.510	0.022
CD4:MDSC	0.460	0.048
CD8:MDSC	0.216	0.375
gMDSC:mMDSC	0.357	0.231
CD4:Treg	0.525	0.017
CD8:Treg	-0.112	0.657

Table 7. Association of effector and memory cells in the tumor with HER2-specific IFNγ response.

Immune cell type		Pearson's or Spearman's r	p-value
% of $CD4^+$ T cells	$\%CD69^+$	-0.436	0.062
	$\%PD\text{-}1^+$	-0.481	0.037
	$\%CD44^-CD62L^+$(naïve)	0.712	0.001
	$\%CD44^-CD62L^-$(EC)	0.120	0.624
	$\%CD44^+CD62L^+$ (T_{CM})	0.565	0.012
	$\%CD44^+$ $CD62L^-$(T_{EM})	-0.553	0.014
	$\%KLRG1^-$ $CD127^-$(EEC)	-0.335	0.161
	$\%KLRG1^-CD127^+$(MPEC)	-0.427	0.069
	$\%KLRG1^+CD127^-$(SLEC)	-0.379	0.110
	$\%KLRG1^+CD127^+$(DPEC)	-0.576	0.017
% of $CD8^+$ T cells	$\%CD69^+$	-0.591	0.008
	$\%PD\text{-}1^+$	-0.569	0.011
	$\%CD44^-CD62L^+$(naïve)	0.668	0.003
	$\%CD44^-CD62L^-$(EC)	0.166	0.497
	$\%CD44^+CD62L^+$ (T_{CM})	0.430	0.066
	$\%CD44^+$ $CD62L^-$(T_{EM})	-0.639	0.003
	$\%KLRG1^-$ $CD127^-$(EEC)	-0.586	0.008
	$\%KLRG1^-CD127^+$(MPEC)	-0.200	0.412
	$\%KLRG1^+CD127^-$(SLEC)	-0.598	0.007
	$\%KLRG1^+CD127^+$(DPEC)	-0.265	0.302

REFERENCES

1. Kasper DL, Harrison TR. Harrison's principles of internal medicine. 16th ed. New York: McGraw-Hill, Medical Pub. Division; 2005.
2. World Cancer Report 2014. Stewart B, Wild C, editors. Lyon: World Health Organization; 2014.
3. Mattiuzzi C, Lippi G. Current Cancer Epidemiology. J Epidemiol Glob Health. 2019;9(4):217-22.
4. Nayak MG, George A, Vidyasagar MS, Mathew S, Nayak S, Nayak BS, et al. Quality of Life among Cancer Patients. Indian J Palliat Care. 2017;23(4):445-50.
5. Cancer Facts & Figures 2021 Atlanta: American Cancer Society; 2021 [Available from: https://www.cancer.org/latest-news/facts-and-figures-2021.html.
6. SEER Cancer Stat Facts: Female Breast Cancer. Bethesda, MD,: National Cancer Institute; 2021 [Available from: https://seer.cancer.gov/statfacts/html/breast.html.
7. Global Cancer Observatory: Cancer Today. Lyon, France: International Agency for Research on Cancer; 2020 [Available from: https://gco.iarc.fr/today.
8. Cunningham DJ, Robinson A. Cunningham's Text-book of anatomy. Rev. 4th ed. New York,: W. Wood and company; 1916. xxvii, 1593 p. p.
9. Last RJ, McMinn RMH. Last's anatomy, regional and applied. 9th ed. Edinburgh ; New York: Churchill Livingstone; 2011. vi, 705 p. p.
10. Ross MH, Pawlina W. Histology : a text and atlas : with correlated cell and molecular biology. 6th ed. Philadelphia: Wolters Kluwer/Lippincott Williams & Wilkins Health; 2011. xviii, 974 p. p.
11. Love SM, Barsky SH. Anatomy of the nipple and breast ducts revisited. Cancer. 2004;101(9):1947-57.
12. Wetstein SC, Onken AM, Luffman C, Baker GM, Pyle ME, Kensler KH, et al. Deep learning assessment of breast terminal duct lobular unit involution: Towards automated prediction of breast cancer risk. PLoS One. 2020;15(4):e0231653.
13. Sims AH, Howell A, Howell SJ, Clarke RB. Origins of breast cancer subtypes and therapeutic implications. Nat Clin Pract Oncol. 2007;4(9):516-25.
14. Makki J. Diversity of Breast Carcinoma: Histological Subtypes and Clinical Relevance. Clin Med Insights Pathol. 2015;8:23-31.
15. Dieci MV, Orvieto E, Dominici M, Conte P, Guarneri V. Rare breast cancer subtypes: histological, molecular, and clinical peculiarities. Oncologist. 2014;19(8):805-13.
16. Rivenbark AG, O'Connor SM, Coleman WB. Molecular and cellular heterogeneity in breast cancer: challenges for personalized medicine. Am J Pathol. 2013;183(4):1113-24.
17. Plichta JK, Campbell BM, Mittendorf EA, Hwang ES. Anatomy and Breast Cancer Staging: Is It Still Relevant? Surg Oncol Clin N Am. 2018;27(1):51-67.
18. Ahmad A. Breast cancer metastasis and drug resistance : progress and prospects. New York: Springer; 2013. xi, 413 pages p.
19. Hulka BS, Moorman PG. Breast cancer: hormones and other risk factors. Maturitas. 2001;38(1):103-13; discussion 13-6.
20. McPherson K, Steel CM, Dixon JM. ABC of breast diseases. Breast cancer-epidemiology, risk factors, and genetics. BMJ. 2000;321(7261):624-8.
21. Henderson IC. Risk factors for breast cancer development. Cancer. 1993;71(6 Suppl):2127-40.
22. Sripan P, Sriplung H, Pongnikorn D, Virani S, Bilheem S, Chaisaengkhaum U, et al. Trends in Female Breast Cancer by Age Group in the Chiang Mai Population. Asian Pac J Cancer Prev. 2017;18(5):1411-6.
23. Anders CK, Johnson R, Litton J, Phillips M, Bleyer A. Breast cancer before age 40 years. Semin Oncol. 2009;36(3):237-49.
24. Sun YS, Zhao Z, Yang ZN, Xu F, Lu HJ, Zhu ZY, et al. Risk Factors and Preventions of Breast Cancer. Int J Biol Sci. 2017;13(11):1387-97.
25. Coughlin SS, Piper M. Genetic polymorphisms and risk of breast cancer. Cancer Epidemiol Biomarkers Prev. 1999;8(11):1023-32.

26. Clavel-Chapelon F, Gerber M. Reproductive factors and breast cancer risk. Do they differ according to age at diagnosis? Breast Cancer Res Treat. 2002;72(2):107-15.
27. MacMahon B, Cole P, Brown J. Etiology of human breast cancer: a review. J Natl Cancer Inst. 1973;50(1):21-42.
28. Mansfield CM. A review of the etiology of breast cancer. J Natl Med Assoc. 1993;85(3):217-21.
29. Linos E, Willett WC. Diet and breast cancer risk reduction. J Natl Compr Canc Netw. 2007;5(8):711-8.
30. Agurs-Collins T, Ross SA, Dunn BK. The Many Faces of Obesity and Its Influence on Breast Cancer Risk. Front Oncol. 2019;9:765.
31. McTiernan A. Weight, physical activity and breast cancer survival. Proc Nutr Soc. 2018;77(4):403-11.
32. Parker ED, Folsom AR. Intentional weight loss and incidence of obesity-related cancers: the Iowa Women's Health Study. Int J Obes Relat Metab Disord. 2003;27(12):1447-52.
33. Rosner B, Eliassen AH, Toriola AT, Chen WY, Hankinson SE, Willett WC, et al. Weight and weight changes in early adulthood and later breast cancer risk. Int J Cancer. 2017;140(9):2003-14.
34. McCawley GM, Ferriss JS, Geffel D, Northup CJ, Modesitt SC. Cancer in obese women: potential protective impact of bariatric surgery. J Am Coll Surg. 2009;208(6):1093-8.
35. de Boer MC, Worner EA, Verlaan D, van Leeuwen PAM. The Mechanisms and Effects of Physical Activity on Breast Cancer. Clin Breast Cancer. 2017;17(4):272-8.
36. Peterson LL, Ligibel JA. Physical Activity and Breast Cancer: an Opportunity to Improve Outcomes. Curr Oncol Rep. 2018;20(7):50.
37. Wu Y, Zhang D, Kang S. Physical activity and risk of breast cancer: a meta-analysis of prospective studies. Breast Cancer Res Treat. 2013;137(3):869-82.
38. Rogers CJ, Colbert LH, Greiner JW, Perkins SN, Hursting SD. Physical activity and cancer prevention : pathways and targets for intervention. Sports Med. 2008;38(4):271-96.
39. Friedenreich CM. Physical activity and breast cancer: review of the epidemiologic evidence and biologic mechanisms. Recent Results Cancer Res. 2011;188:125-39.
40. Irwin ML, Varma K, Alvarez-Reeves M, Cadmus L, Wiley A, Chung GG, et al. Randomized controlled trial of aerobic exercise on insulin and insulin-like growth factors in breast cancer survivors: the Yale Exercise and Survivorship study. Cancer Epidemiol Biomarkers Prev. 2009;18(1):306-13.
41. Fairey AS, Courneya KS, Field CJ, Bell GJ, Jones LW, Mackey JR. Randomized controlled trial of exercise and blood immune function in postmenopausal breast cancer survivors. J Appl Physiol (1985). 2005;98(4):1534-40.
42. Xu Y, Rogers CJ. Impact of physical activity and energy restriction on immune regulation of cancer. Translational Cancer Research. 2020;9(9):5700-31.
43. Turbitt WJ, Xu Y, Sosnoski DM, Collins SD, Meng H, Mastro AM, et al. Physical Activity Plus Energy Restriction Prevents 4T1.2 Mammary Tumor Progression, MDSC Accumulation, and an Immunosuppressive Tumor Microenvironment. Cancer Prev Res (Phila). 2019;12(8):493-506.
44. Harvie M, Howell A. Energy restriction and the prevention of breast cancer. Proc Nutr Soc. 2012;71(2):263-75.
45. Harvie M, Howell A. Energy balance adiposity and breast cancer - energy restriction strategies for breast cancer prevention. Obes Rev. 2006;7(1):33-47.
46. Maughan KL, Lutterbie MA, Ham PS. Treatment of breast cancer. Am Fam Physician. 2010;81(11):1339-46.
47. Waks AG, Winer EP. Breast Cancer Treatment: A Review. JAMA. 2019;321(3):288-300.
48. Moreno Ayala MA, Gottardo MF, Asad AS, Zuccato C, Nicola A, Seilicovich A, et al. Immunotherapy for the treatment of breast cancer. Expert Opin Biol Ther. 2017;17(7):797-812.

49. Garcia-Aranda M, Redondo M. Immunotherapy: A Challenge of Breast Cancer Treatment. Cancers (Basel). 2019;11(12).
50. Soliman H. Immunotherapy strategies in the treatment of breast cancer. Cancer Control. 2013;20(1):17-21.
51. Ernst B, Anderson KS. Immunotherapy for the treatment of breast cancer. Curr Oncol Rep. 2015;17(2):5.
52. Murphy K, Weaver C. Janeway's immunobiology. 9th edition. ed. New York, NY: Garland Science/Taylor & Francis Group, LLC; 2016. xx, 904 pages p.
53. Kennedy MA. A brief review of the basics of immunology: the innate and adaptive response. Vet Clin North Am Small Anim Pract. 2010;40(3):369-79.
54. Rezaei N. Cancer Immunology : A Translational Medicine Context. Berlin, Heidelberg: Springer Berlin Heidelberg : Imprint: Springer,; 2015.
55. Chaplin DD. Overview of the immune response. J Allergy Clin Immunol. 2010;125(2 Suppl 2):S3-23.
56. Pastula A, Marcinkiewicz J. Myeloid-derived suppressor cells: a double-edged sword? Int J Exp Pathol. 2011;92(2):73-8.
57. Mosser DM, Edwards JP. Exploring the full spectrum of macrophage activation. Nat Rev Immunol. 2008;8(12):958-69.
58. Vivier E, Tomasello E, Baratin M, Walzer T, Ugolini S. Functions of natural killer cells. Nat Immunol. 2008;9(5):503-10.
59. Weinberg RA. The biology of cancer. Second edition. ed. New York: Garland Science, Taylor & Francis Group; 2014. xx, 876, A 6, G 30, I 28 pages p.
60. Frauwirth KA, Thompson CB. Activation and inhibition of lymphocytes by costimulation. J Clin Invest. 2002;109(3):295-9.
61. Engels EA. Epidemiologic perspectives on immunosuppressed populations and the immunosurveillance and immunocontainment of cancer. Am J Transplant. 2019;19(12):3223-32.
62. Dalgleish AG, Haefner B. The link between inflammation and cancer : wounds that do not heal. New York, NY: Springer; 2006. xii, 254 p. p.
63. Lei X, Lei Y, Li JK, Du WX, Li RG, Yang J, et al. Immune cells within the tumor microenvironment: Biological functions and roles in cancer immunotherapy. Cancer Lett. 2020;470:126-33.
64. Farhood B, Najafi M, Mortezaee K. CD8(+) cytotoxic T lymphocytes in cancer immunotherapy: A review. J Cell Physiol. 2019;234(6):8509-21.
65. Morvan MG, Lanier LL. NK cells and cancer: you can teach innate cells new tricks. Nat Rev Cancer. 2016;16(1):7-19.
66. Wculek SK, Cueto FJ, Mujal AM, Melero I, Krummel MF, Sancho D. Dendritic cells in cancer immunology and immunotherapy. Nat Rev Immunol. 2020;20(1):7-24.
67. Gardner A, Ruffell B. Dendritic Cells and Cancer Immunity. Trends Immunol. 2016;37(12):855-65.
68. Veglia F, Gabrilovich DI. Dendritic cells in cancer: the role revisited. Curr Opin Immunol. 2017;45:43-51.
69. Kim HJ, Cantor H. CD4 T-cell subsets and tumor immunity: the helpful and the not-so-helpful. Cancer Immunol Res. 2014;2(2):91-8.
70. Gerloni M, Zanetti M. CD4 T cells in tumor immunity. Springer Semin Immunopathol. 2005;27(1):37-48.
71. Zhou J, Tang Z, Gao S, Li C, Feng Y, Zhou X. Tumor-Associated Macrophages: Recent Insights and Therapies. Front Oncol. 2020;10:188.
72. Salmaninejad A, Valilou SF, Soltani A, Ahmadi S, Abarghan YJ, Rosengren RJ, et al. Tumor-associated macrophages: role in cancer development and therapeutic implications. Cell Oncol (Dordr). 2019;42(5):591-608.
73. Cassetta L, Pollard JW. Targeting macrophages: therapeutic approaches in cancer. Nat Rev Drug Discov. 2018;17(12):887-904.
74. Ostuni R, Kratochvill F, Murray PJ, Natoli G. Macrophages and cancer: from mechanisms to therapeutic implications. Trends Immunol. 2015;36(4):229-39.

75. Qiu SQ, Waaijer SJH, Zwager MC, de Vries EGE, van der Vegt B, Schroder CP. Tumor-associated macrophages in breast cancer: Innocent bystander or important player? Cancer Treat Rev. 2018;70:178-89.
76. Whiteside TL. Regulatory T cell subsets in human cancer: are they regulating for or against tumor progression? Cancer Immunol Immunother. 2014;63(1):67-72.
77. Dees S, Ganesan R, Singh S, Grewal IS. Regulatory T cell targeting in cancer: Emerging strategies in immunotherapy. Eur J Immunol. 2021;51(2):280-91.
78. Ward-Hartstonge KA, Kemp RA. Regulatory T-cell heterogeneity and the cancer immune response. Clin Transl Immunology. 2017;6(9):e154.
79. Lim HX, Kim TS, Poh CL. Understanding the Differentiation, Expansion, Recruitment and Suppressive Activities of Myeloid-Derived Suppressor Cells in Cancers. Int J Mol Sci. 2020;21(10).
80. Gabrilovich DI, Nagaraj S. Myeloid-derived suppressor cells as regulators of the immune system. Nat Rev Immunol. 2009;9(3):162-74.
81. Wynn TA. Myeloid-cell differentiation redefined in cancer. Nat Immunol. 2013;14(3):197-9.
82. Pyzer AR, Cole L, Rosenblatt J, Avigan DE. Myeloid-derived suppressor cells as effectors of immune suppression in cancer. Int J Cancer. 2016;139(9):1915-26.
83. Talmadge JE. Pathways mediating the expansion and immunosuppressive activity of myeloid-derived suppressor cells and their relevance to cancer therapy. Clin Cancer Res. 2007;13(18 Pt 1):5243-8.
84. Ostrand-Rosenberg S, Sinha P. Myeloid-derived suppressor cells: linking inflammation and cancer. J Immunol. 2009;182(8):4499-506.
85. Stovgaard ES, Nielsen D, Hogdall E, Balslev E. Triple negative breast cancer - prognostic role of immune-related factors: a systematic review. Acta Oncol. 2018;57(1):74-82.
86. Burugu S, Asleh-Aburaya K, Nielsen TO. Immune infiltrates in the breast cancer microenvironment: detection, characterization and clinical implication. Breast Cancer. 2017;24(1):3-15.
87. Disis ML, Stanton SE. Triple-negative breast cancer: immune modulation as the new treatment paradigm. Am Soc Clin Oncol Educ Book. 2015:e25-30.
88. Ali HR, Provenzano E, Dawson SJ, Blows FM, Liu B, Shah M, et al. Association between CD8+ T-cell infiltration and breast cancer survival in 12,439 patients. Ann Oncol. 2014;25(8):1536-43.
89. Mahmoud SM, Paish EC, Powe DG, Macmillan RD, Grainge MJ, Lee AH, et al. Tumor-infiltrating CD8+ lymphocytes predict clinical outcome in breast cancer. J Clin Oncol. 2011;29(15):1949-55.
90. Gu-Trantien C, Loi S, Garaud S, Equeter C, Libin M, de Wind A, et al. CD4(+) follicular helper T cell infiltration predicts breast cancer survival. J Clin Invest. 2013;123(7):2873-92.
91. Matikas A, Zerdes I, Lovrot J, Richard F, Sotiriou C, Bergh J, et al. Prognostic Implications of PD-L1 Expression in Breast Cancer: Systematic Review and Meta-analysis of Immunohistochemistry and Pooled Analysis of Transcriptomic Data. Clin Cancer Res. 2019;25(18):5717-26.
92. Botti G, Collina F, Scognamiglio G, Rao F, Peluso V, De Cecio R, et al. Programmed Death Ligand 1 (PD-L1) Tumor Expression Is Associated with a Better Prognosis and Diabetic Disease in Triple Negative Breast Cancer Patients. Int J Mol Sci. 2017;18(2).
93. Wang ZQ, Milne K, Derocher H, Webb JR, Nelson BH, Watson PH. PD-L1 and intratumoral immune response in breast cancer. Oncotarget. 2017;8(31):51641-51.
94. Mori H, Kubo M, Yamaguchi R, Nishimura R, Osako T, Arima N, et al. The combination of PD-L1 expression and decreased tumor-infiltrating lymphocytes is associated with a poor prognosis in triple-negative breast cancer. Oncotarget. 2017;8(9):15584-92.
95. Zhang M, Sun H, Zhao S, Wang Y, Pu H, Wang Y, et al. Expression of PD-L1 and prognosis in breast cancer: a meta-analysis. Oncotarget. 2017;8(19):31347-54.

96. Yeong J, Thike AA, Lim JC, Lee B, Li H, Wong SC, et al. Higher densities of Foxp3(+) regulatory T cells are associated with better prognosis in triple-negative breast cancer. Breast Cancer Res Treat. 2017;163(1):21-35.
97. West NR, Kost SE, Martin SD, Milne K, Deleeuw RJ, Nelson BH, et al. Tumour-infiltrating FOXP3(+) lymphocytes are associated with cytotoxic immune responses and good clinical outcome in oestrogen receptor-negative breast cancer. Br J Cancer. 2013;108(1):155-62.
98. Hinshaw DC, Shevde LA. The Tumor Microenvironment Innately Modulates Cancer Progression. Cancer Res. 2019;79(18):4557-66.
99. Ascierto ML, Idowu MO, Zhao Y, Khalak H, Payne KK, Wang XY, et al. Molecular signatures mostly associated with NK cells are predictive of relapse free survival in breast cancer patients. J Transl Med. 2013;11:145.
100. Bronte V, Brandau S, Chen SH, Colombo MP, Frey AB, Greten TF, et al. Recommendations for myeloid-derived suppressor cell nomenclature and characterization standards. Nat Commun. 2016;7:12150.
101. Umansky V, Blattner C, Gebhardt C, Utikal J. The Role of Myeloid-Derived Suppressor Cells (MDSC) in Cancer Progression. Vaccines (Basel). 2016;4(4).
102. Diaz-Montero CM, Salem ML, Nishimura MI, Garrett-Mayer E, Cole DJ, Montero AJ. Increased circulating myeloid-derived suppressor cells correlate with clinical cancer stage, metastatic tumor burden, and doxorubicin-cyclophosphamide chemotherapy. Cancer Immunol Immunother. 2009;58(1):49-59.
103. Kim IS, Baek SH. Mouse models for breast cancer metastasis. Biochem Biophys Res Commun. 2010;394(3):443-7.
104. Khanna C, Hunter K. Modeling metastasis in vivo. Carcinogenesis. 2005;26(3):513-23.
105. Park MK, Lee CH, Lee H. Mouse models of breast cancer in preclinical research. Lab Anim Res. 2018;34(4):160-5.
106. Takizawa Y, Saida T, Tokuda Y, Dohi S, Wang YL, Urano K, et al. New immunodeficient (nude-scid, beige-scid) mice as excellent recipients of human skin grafts containing intraepidermal neoplasms. Arch Dermatol Res. 1997;289(4):213-8.
107. Kretschmann KL, Welm AL. Mouse models of breast cancer metastasis to bone. Cancer Metastasis Rev. 2012;31(3-4):579-83.
108. Aslakson CJ, Miller FR. Selective events in the metastatic process defined by analysis of the sequential dissemination of subpopulations of a mouse mammary tumor. Cancer Res. 1992;52(6):1399-405.
109. Lelekakis M, Moseley JM, Martin TJ, Hards D, Williams E, Ho P, et al. A novel orthotopic model of breast cancer metastasis to bone. Clin Exp Metastasis. 1999;17(2):163-70.
110. Johnstone CN, Smith YE, Cao Y, Burrows AD, Cross RS, Ling X, et al. Functional and molecular characterisation of EO771.LMB tumours, a new C57BL/6-mouse-derived model of spontaneously metastatic mammary cancer. Dis Model Mech. 2015;8(3):237-51.
111. Eckhardt BL, Parker BS, van Laar RK, Restall CM, Natoli AL, Tavaria MD, et al. Genomic analysis of a spontaneous model of breast cancer metastasis to bone reveals a role for the extracellular matrix. Mol Cancer Res. 2005;3(1):1-13.
112. Liu Y, Wang H, Zhao J, Ma J, Wei L, Wu S, et al. Enhancement of immunogenicity of tumor cells by cotransfection with genes encoding antisense insulin-like growth factor-1 and B7.1 molecules. Cancer Gene Ther. 2000;7(3):456-65.
113. Nilofar Danishmalik S, Lee SH, Sin JI. Tumor regression is mediated via the induction of HER263-71- specific CD8+ CTL activity in a 4T1.2/HER2 tumor model: no involvement of CD80 in tumor control. Oncotarget. 2017;8(16):26771-88.
114. Kershaw MH, Jackson JT, Haynes NM, Teng MW, Moeller M, Hayakawa Y, et al. Gene-engineered T cells as a superior adjuvant therapy for metastatic cancer. J Immunol. 2004;173(3):2143-50.

115. Xu Y, Rogers CJ. Temporal changes in immune responses within the tumor microenvironment in the 4T1.2-HER2 mammary tumor model Breast Cancer Research (submitted). 2021.
116. Pulaski BA, Ostrand-Rosenberg S. Reduction of established spontaneous mammary carcinoma metastases following immunotherapy with major histocompatibility complex class II and B7.1 cell-based tumor vaccines. Cancer Res. 1998;58(7):1486-93.
117. Turbitt WJ, Black AJ, Collins SD, Meng H, Xu H, Washington S, et al. Fish Oil Enhances T Cell Function and Tumor Infiltration and Is Correlated With a Cancer Prevention Effect in HER-2/neu But Not PyMT Transgenic Mice. Nutr Cancer. 2015;67(6):965-75.
118. Lian J, Yue Y, Yu W, Zhang Y. Immunosenescence: a key player in cancer development. J Hematol Oncol. 2020;13(1):151.
119. Oh J, Magnuson A, Benoist C, Pittet MJ, Weissleder R. Age-related tumor growth in mice is related to integrin alpha 4 in CD8+ T cells. JCI Insight. 2018;3(21).
120. Drijvers JM, Sharpe AH, Haigis MC. The effects of age and systemic metabolism on anti-tumor T cell responses. Elife. 2020;9.
121. Haseman JK, Bourbina J, Eustis SL. Effect of individual housing and other experimental design factors on tumor incidence in B6C3F1 mice. Fundam Appl Toxicol. 1994;23(1):44-52.
122. Williamson CM, Lee W, DeCasien AR, Lanham A, Romeo RD, Curley JP. Social hierarchy position in female mice is associated with plasma corticosterone levels and hypothalamic gene expression. Sci Rep. 2019;9(1):7324.
123. Bartolomucci A, Palanza P, Gaspani L, Limiroli E, Panerai AE, Ceresini G, et al. Social status in mice: behavioral, endocrine and immune changes are context dependent. Physiol Behav. 2001;73(3):401-10.
124. Schuhr B. Social structure and plasma corticosterone level in female albino mice. Physiol Behav. 1987;40(6):689-93.
125. Lee JY, Murphy SM, Scanlon EF. Effect of trauma on implantation of metastatic tumor in bone in mice. J Surg Oncol. 1994;56(3):178-84.
126. El Saghir NS, Elhajj, II, Geara FB, Hourani MH. Trauma-associated growth of suspected dormant micrometastasis. BMC Cancer. 2005;5:94.
127. Haseman JK, Huff JE, Rao GN, Eustis SL. Sources of variability in rodent carcinogenicity studies. Fundam Appl Toxicol. 1989;12(4):793-804.
128. Angell TE, Lechner MG, Jang JK, LoPresti JS, Epstein AL. MHC class I loss is a frequent mechanism of immune escape in papillary thyroid cancer that is reversed by interferon and selumetinib treatment in vitro. Clin Cancer Res. 2014;20(23):6034-44.
129. Lee SY, Sin JI. MC32 tumor cells acquire Ag-specific CTL resistance through the loss of CEA in a colon cancer model. Hum Vaccin Immunother. 2015;11(8):2012-20.
130. Han BS, Ji S, Woo S, Lee JH, Sin JI. Regulation of the translation activity of antigen-specific mRNA is responsible for antigen loss and tumor immune escape in a HER2-expressing tumor model. Sci Rep. 2019;9(1):2855.
131. Tran Janco JM, Lamichhane P, Karyampudi L, Knutson KL. Tumor-infiltrating dendritic cells in cancer pathogenesis. J Immunol. 2015;194(7):2985-91.
132. Sisirak V, Faget J, Gobert M, Goutagny N, Vey N, Treilleux I, et al. Impaired IFN-alpha production by plasmacytoid dendritic cells favors regulatory T-cell expansion that may contribute to breast cancer progression. Cancer Res. 2012;72(20):5188-97.
133. Foulds GA, Vadakekolathu J, Abdel-Fatah TMA, Nagarajan D, Reeder S, Johnson C, et al. Immune-Phenotyping and Transcriptomic Profiling of Peripheral Blood Mononuclear Cells From Patients With Breast Cancer: Identification of a 3 Gene Signature Which Predicts Relapse of Triple Negative Breast Cancer. Front Immunol. 2018;9:2028.
134. Markowitz J, Wesolowski R, Papenfuss T, Brooks TR, Carson WE, 3rd. Myeloid-derived suppressor cells in breast cancer. Breast Cancer Res Treat. 2013;140(1):13-21.
135. Youn JI, Nagaraj S, Collazo M, Gabrilovich DI. Subsets of myeloid-derived suppressor cells in tumor-bearing mice. J Immunol. 2008;181(8):5791-802.
136. Kumar V, Patel S, Tcyganov E, Gabrilovich DI. The Nature of Myeloid-Derived Suppressor Cells in the Tumor Microenvironment. Trends Immunol. 2016;37(3):208-20.

137. Klebanoff CA, Gattinoni L, Torabi-Parizi P, Kerstann K, Cardones AR, Finkelstein SE, et al. Central memory self/tumor-reactive CD8+ T cells confer superior antitumor immunity compared with effector memory T cells. Proc Natl Acad Sci U S A. 2005;102(27):9571-6.
138. Wang X, Berger C, Wong CW, Forman SJ, Riddell SR, Jensen MC. Engraftment of human central memory-derived effector CD8+ T cells in immunodeficient mice. Blood. 2011;117(6):1888-98.
139. Liu Q, Sun Z, Chen L. Memory T cells: strategies for optimizing tumor immunotherapy. Protein Cell. 2020;11(8):549-64.
140. Pages F, Kirilovsky A, Mlecnik B, Asslaber M, Tosolini M, Bindea G, et al. In situ cytotoxic and memory T cells predict outcome in patients with early-stage colorectal cancer. J Clin Oncol. 2009;27(35):5944-51.
141. Egelston CA, Avalos C, Tu TY, Rosario A, Wang R, Solomon S, et al. Resident memory CD8+ T cells within cancer islands mediate survival in breast cancer patients. JCI Insight. 2019;4(19).
142. Romero-Cordoba S, Meneghini E, Sant M, Iorio MV, Sfondrini L, Paolini B, et al. Decoding Immune Heterogeneity of Triple Negative Breast Cancer and Its Association with Systemic Inflammation. Cancers (Basel). 2019;11(7).
143. Scrimieri F, Askew D, Corn DJ, Eid S, Bobanga ID, Bjelac JA, et al. Murine leukemia virus envelope gp70 is a shared biomarker for the high-sensitivity quantification of murine tumor burden. Oncoimmunology. 2013;2(11):e26889.